Beyond Landau Fermi liquid and BCS superconductivity near quantum criticality

Hilbert v. Löhneysen

Physikalisches Institut and Institut für Festkörperphysik
Karlsruhe Institute of Technology

Lecture Series at APCTP, Pohang

May 23-27, 2016

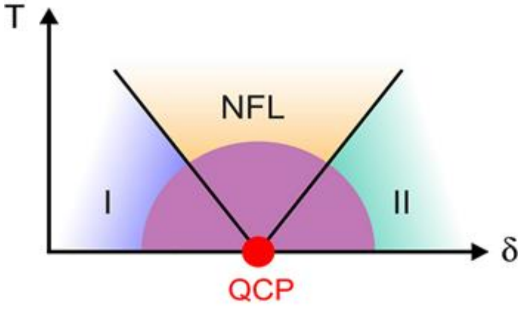

Karlsruhe Institute of Technology

Lecture 3
$CeCu_{6-x}Au_x$ – a case study for quantum criticality in heavy fermion systems

Contents of Lecture 3

Introduction to the $CeCu_{6-x}Au_x$ system

Non-Fermi-liquid thermodynamic and transport properties

Measurement of critical fluctuations by inelastic neutron scattering

Fate of the Kondo energy scale

at the concentration-tuned QCPin $CeCu_{6-x}Au_x$?

Role of the tuning parameter:

compositon, hydrostatic pressure, magnetic field

Determining the entropy landscape near quantum criticality

Does the monoclinic-orthorhombic transition qualify as a QPT?

Introduction to the $CeCu_{6-x}Au_x$ system

Heavy-fermion system $CeCu_6$

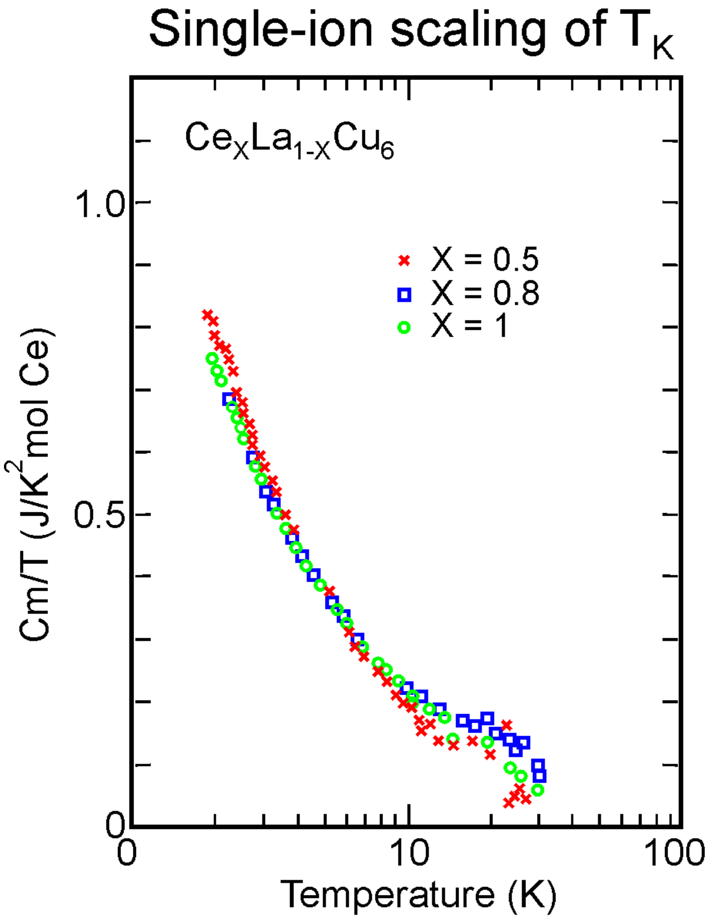

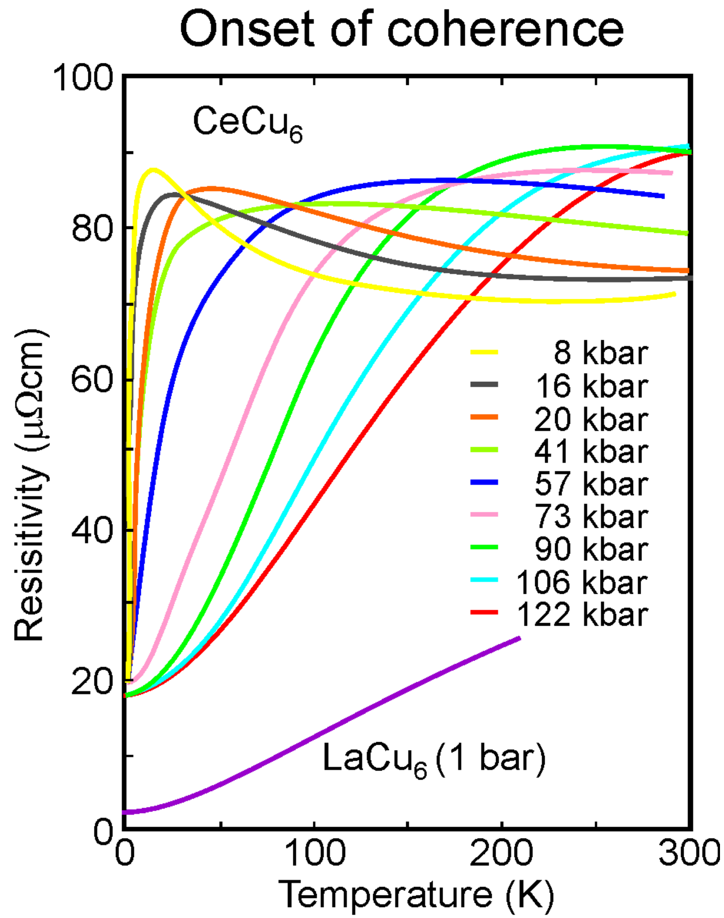

Onuki, Komatsubara

Note: evidence for magnetic order in $CeCu_6$ at $T \sim$ 3 mK

*E. A. Schuberth et al, PRB **51**, 12892 (1995)*

Magnetic order in $CeCu_{6-x}Au_x$

$CeCu_6$: heavy fermions with $\gamma = 1.6$ J/molK^2

non-magnetic groundstate

Ōnuki et al., Amato et al.

short lived AF correlations

Aeppli et al., Rossat-Mignod et al.

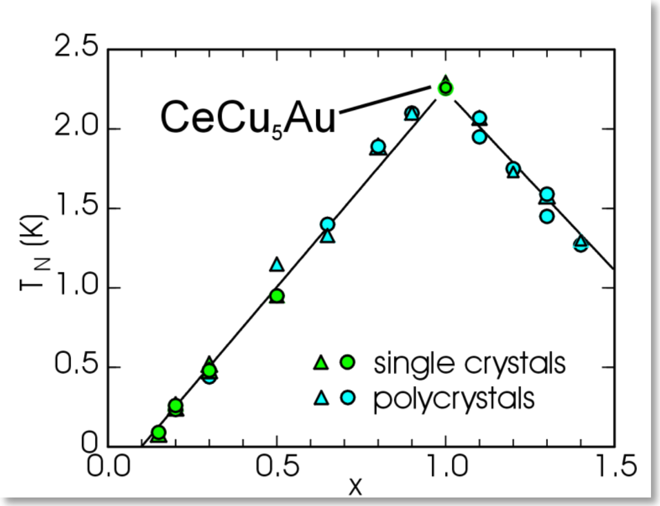

Alloying with Au: long-range AF order

"negative lattice pressure" explains $T_N(x)$ for $x < 1$

Direct proof: Néel temperature T_N vanishes under hydrostatic pressure

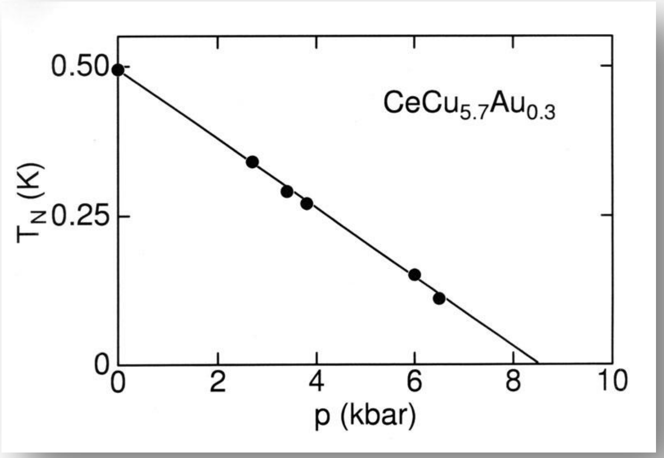

x = 0.1: Quantum critical point with "non-Fermi liquid" behavior

Crystal structure and magnetic order of $CeCu_{6-x}Au_x$

Orthorhombic structure
Pnma

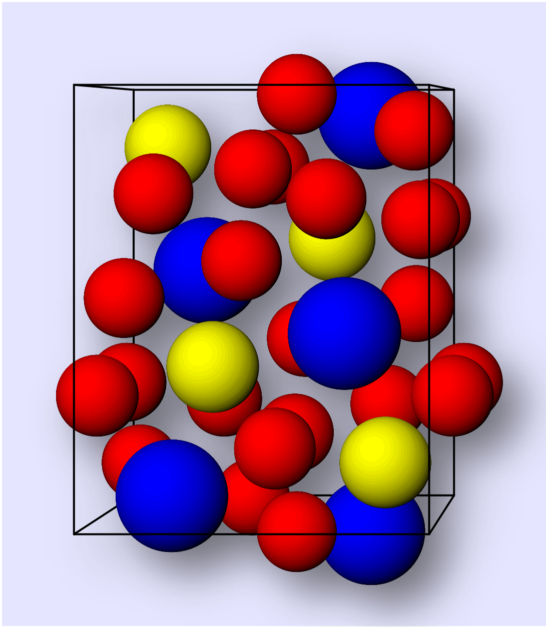

Incommensurate three-dimensional magnetic ordering ...

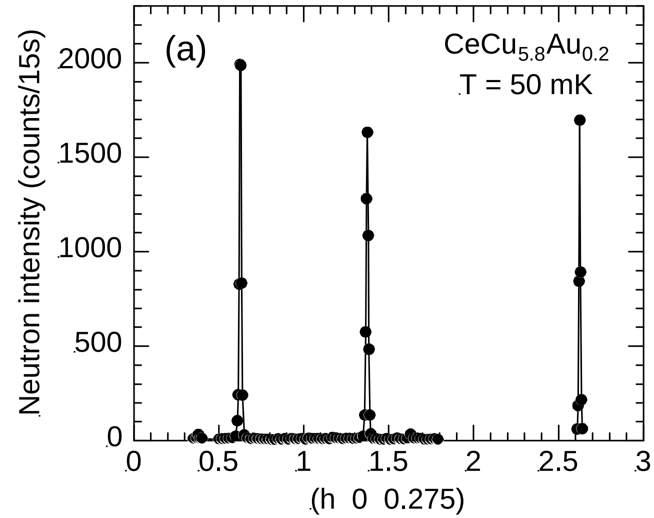

... confined to the *a*c** plane, *c** component depends on x

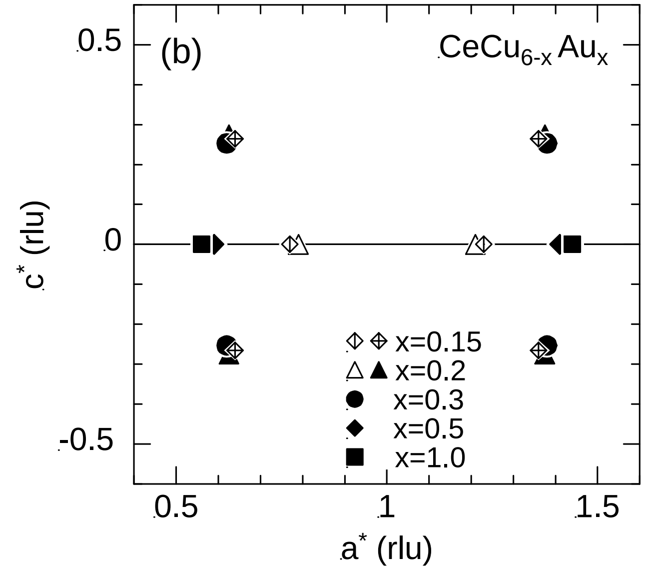

$CeCu_6$:
small monoclinic distortion suppressed for $x > 0.15$

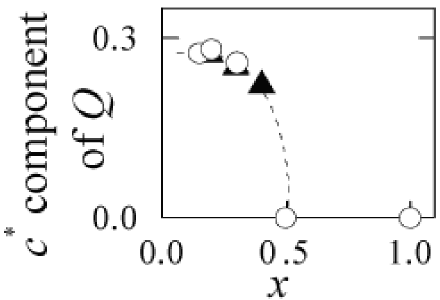

Crystal growth of $CeCu_{6-x}Au_x$ crystals

Czochralski method

Pulling from the melt in a W crucible
inductive heating
Ar pressure (p = 2.5 bar)

Starting materials:
Ce (4N), Cu (5N), Au (5N)

Pulling speed: 12 – 20 mm/h
rotation: 3-5 min^{-1}

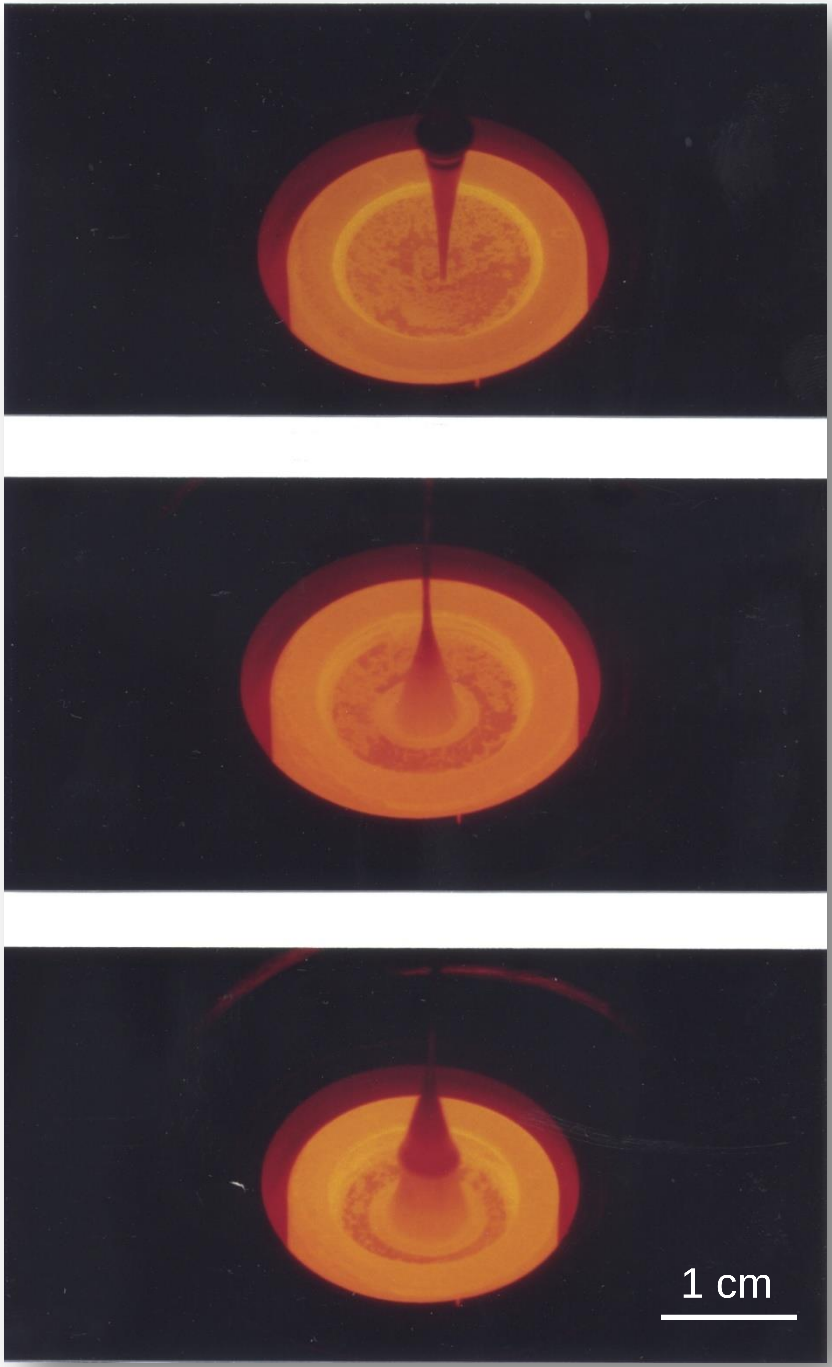

Non-Fermi-liquid thermodynamic and properties in $CeCu_{6-x}Au_x$ near the quantum critical point $x = 0.1$

Non-Fermi liquid effects at quantum critical point in $CeCu_{6-x}Au_x$

Specific heat

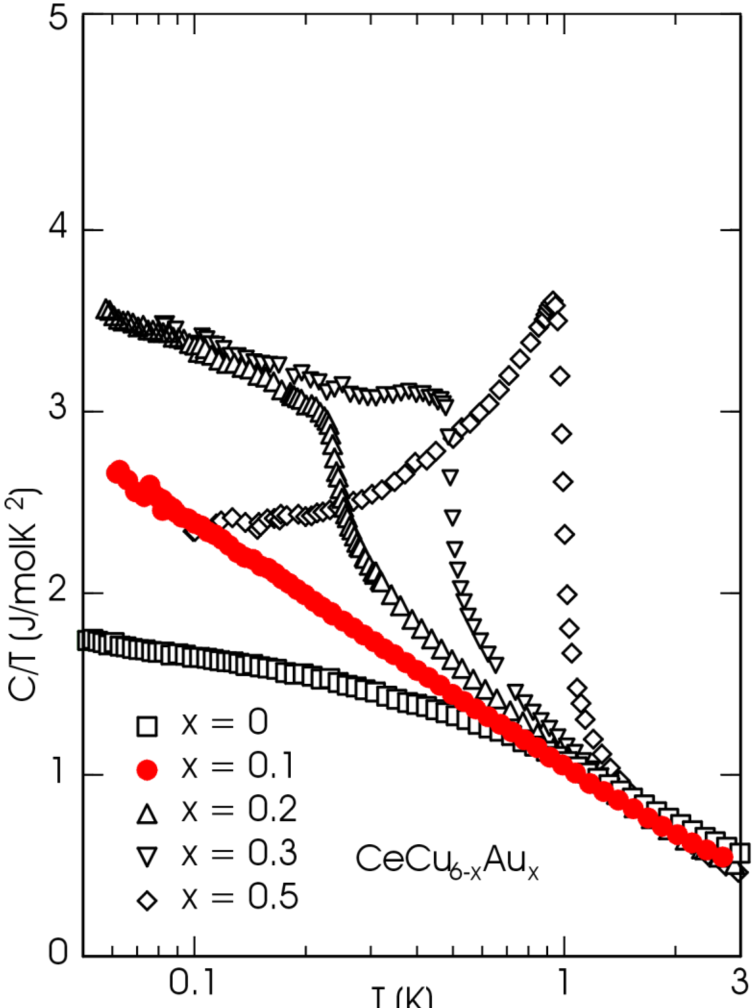

Electrical resistivity

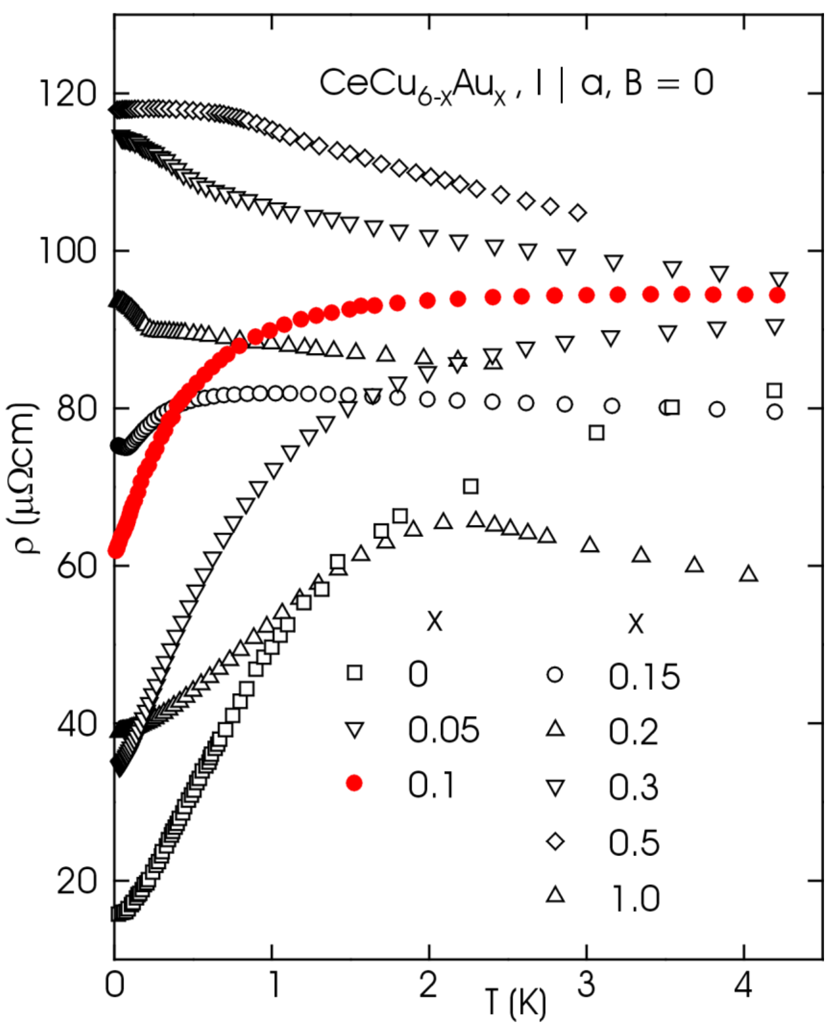

Measurement of quantum-critical fluctuations by inelastic neutron scattering

Neutron scattering

$$S(\underline{Q},\omega) \sim \sum_{i,j} \int e^{i\underline{Q}(\underline{R}_i - \underline{R}_j)} \langle \underline{J}_i(0)\,\underline{J}_j(t) \rangle e^{-i\omega t} dt$$

spin-spin correlation function

$$S(\underline{Q},\omega = \text{const}) \sim \frac{1}{\xi^{-2} + (\underline{Q} - \underline{Q}_0)^2}$$

$$S(Q = \text{const},\omega) \sim \frac{1}{1 - e^{-\hbar\omega/kT}} \frac{\omega\,\Gamma/2}{(\Gamma/2)^2 + \omega^2}$$

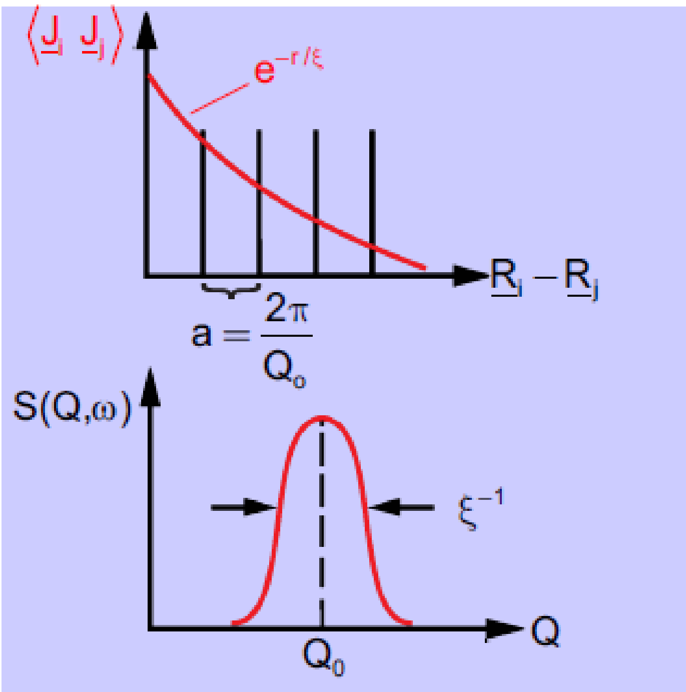

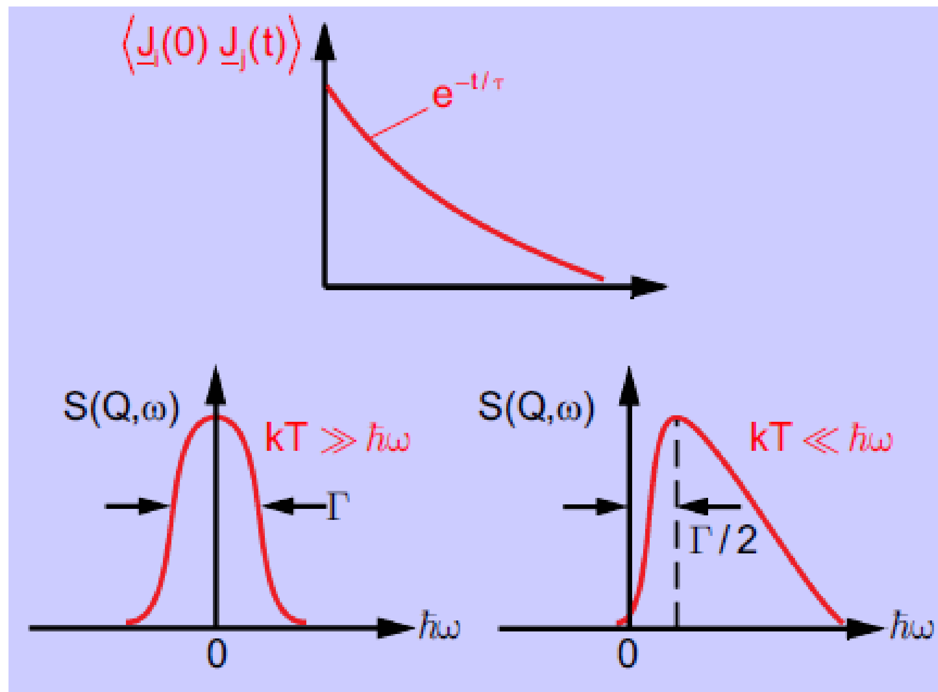

Inelastic neutron scattering intensity of $CeCu_{5.9}Au_{0.1}$

Scans along c* in the *a*c** plane

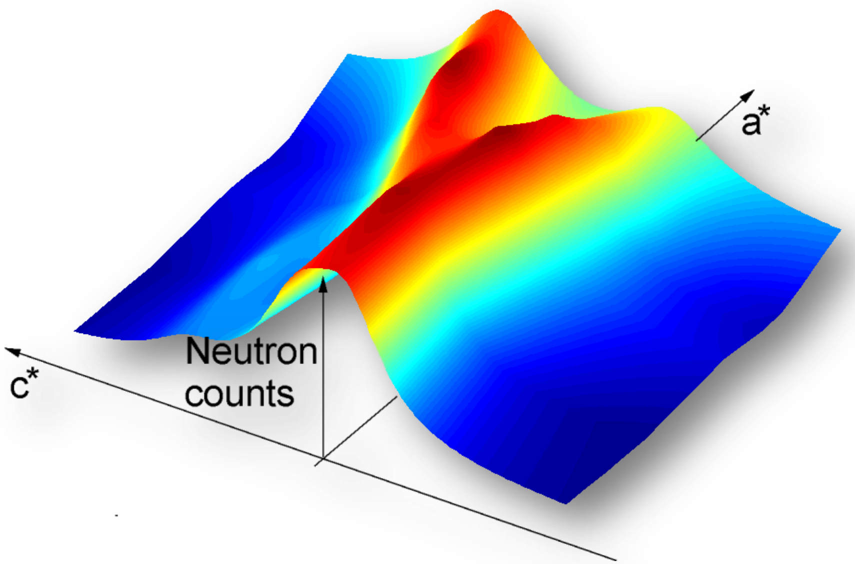

energy transfer $\hbar\omega = 0.1$ meV

ILL, IN 14

O. Stockert et al., PRL 1998

1D features in k-space equivalent to

2D features in real space

$\Rightarrow$ quasi-2D fluctuations

Coupling to 3D quasiparticles

$d = 2$, $z = 2$

$\Rightarrow$ $d_{\text{eff}} = d + z = 4$

Spin-density wave scenario:

$$\frac{C}{T} = a \ln\left(\frac{T_0}{T}\right), \quad \Delta\rho \sim T$$

$$T_N \sim |\delta - \delta_C|, \quad \delta = p, x$$

Hertz, Millis, Moriya, Lonzarich, Rosch

Inelastic neutron scattering intensity in the a*c* plane

x = 0   x = 0.1   x = 0.2

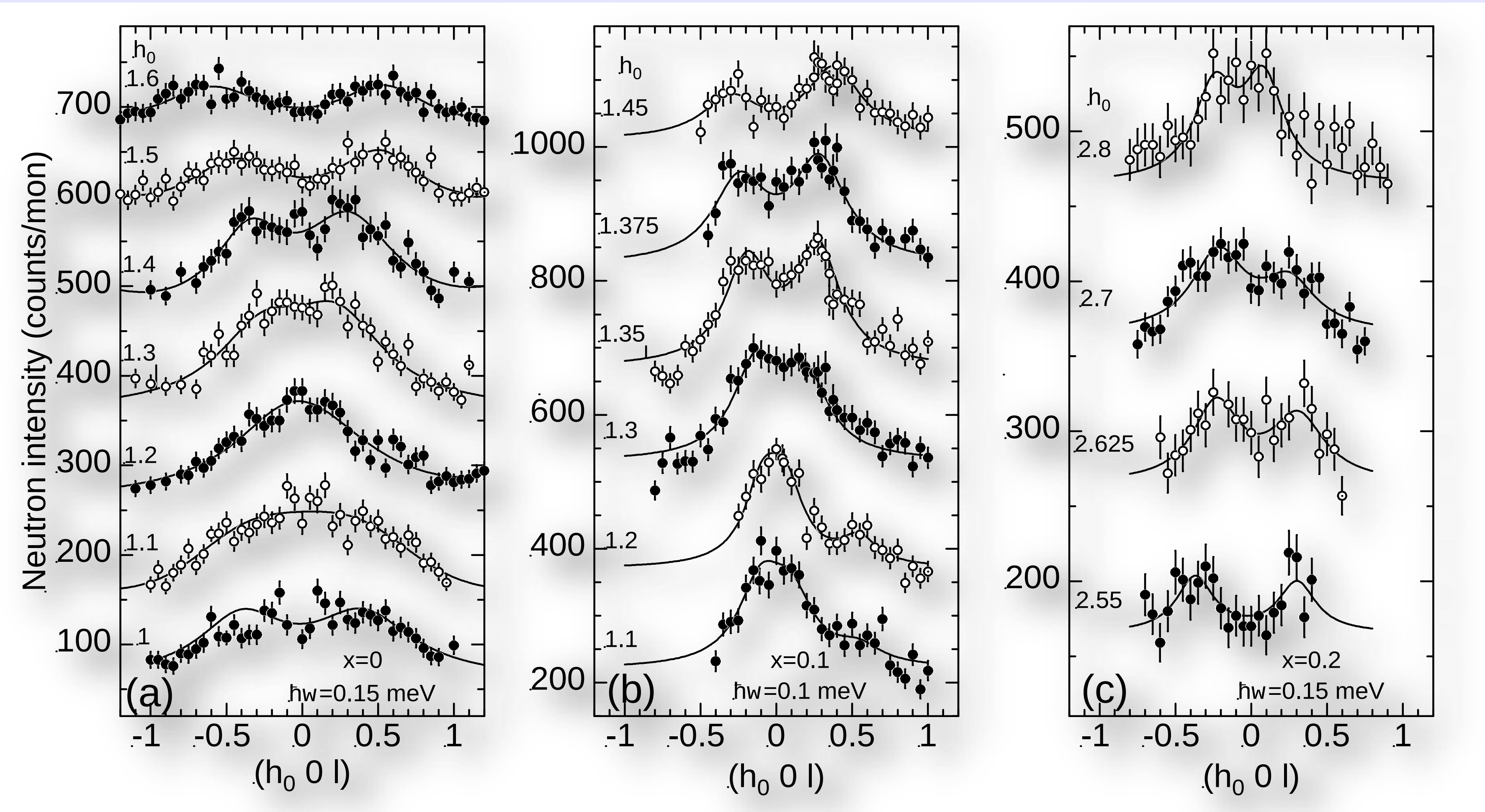

Dynamical scaling of magnetic fluctuations in $CeCu_{6-x}Au_x$

A. Schröder et al., Nature 2000

Scaling of the dynamical susceptibility of critical fluctuations for $x = 0.1 \approx x_c$, with ω/T, independent of q, with anomalous scaling exponent $\alpha = 0.75$

incompatible with Hertz-Millis-Moriya model which predicts $\omega/T^{1.5}$ scaling and. $\alpha = 1$.

Further, the scaling is observed (with reduced amplitude) in various points of the Brillouin zone, not only at the wavevectorof incommensurate order

→ „local quantum criticality

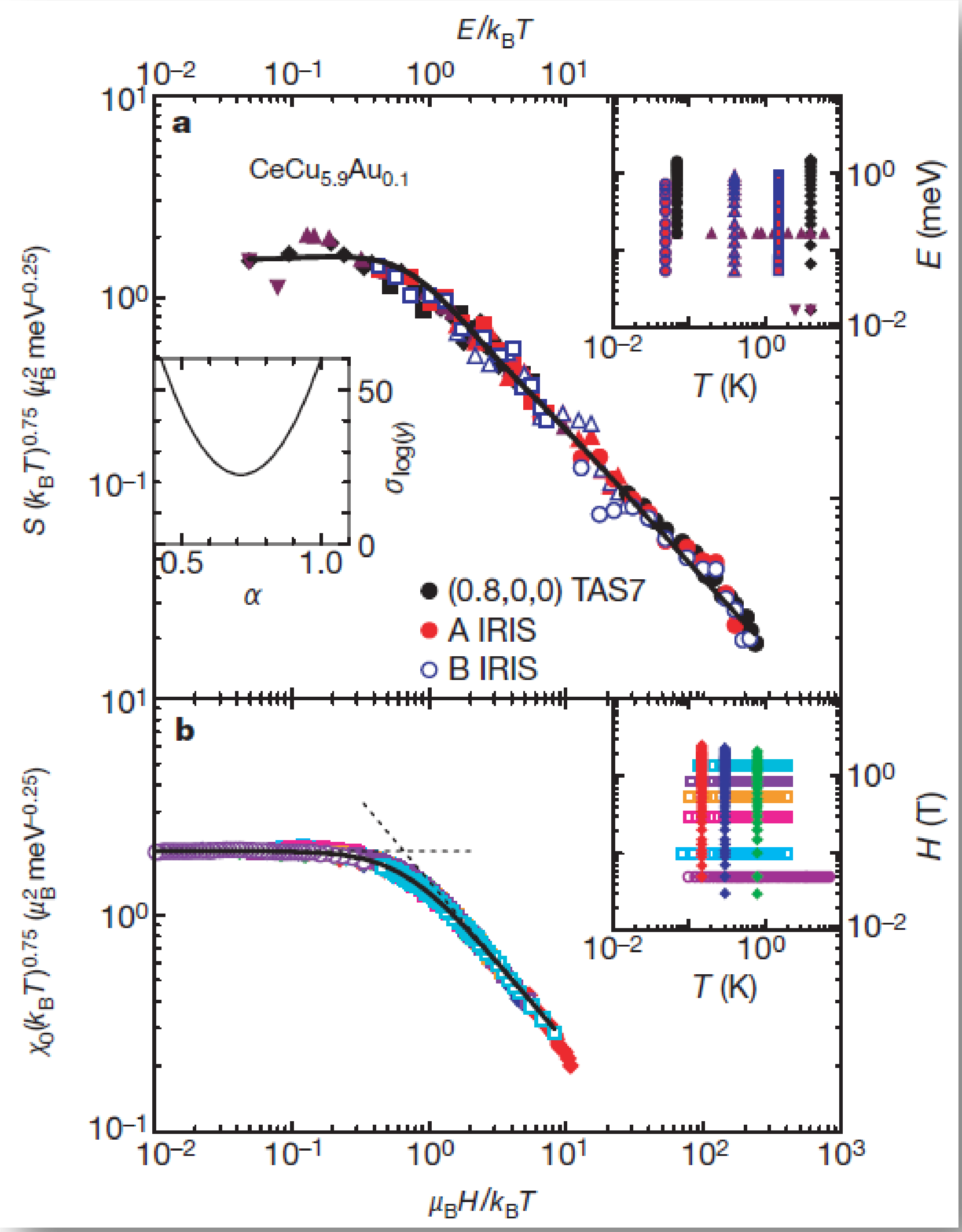

Fate of the Kondo energy scale at the concentration-tuned QCP in $CeCu_{6-x}Au_x$?

Fermi-volume change due to Kondo collapse at the onset of magnetic ordering?

$YbRh_2Si_2$: moderately heavy effective masses.

magnetic transition at 70 mK can be suppressed by an small magnetic field

Specific heat

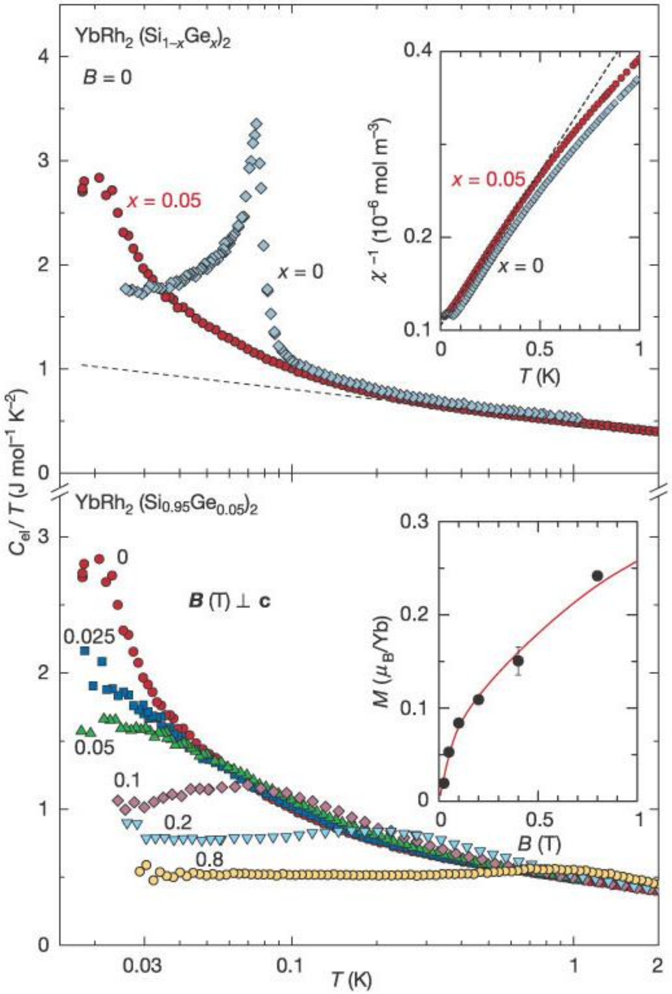

J. Custers et al., Nature 2003

(B,T) phase diagram

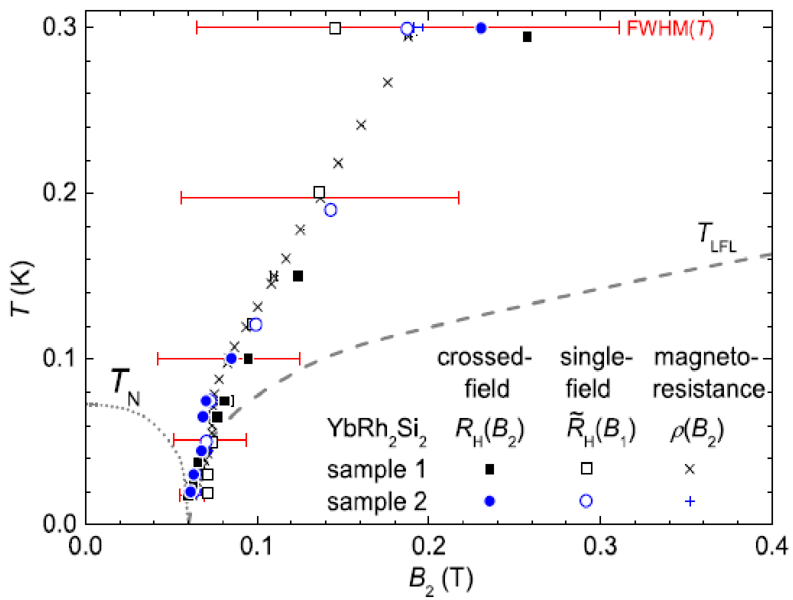

S. Paschen et al., Nature 2005
S. Fríedemann et al., PNAS 2010

Additional line T^* emenating from CCP

Strong change in Hall constant of $YbRh_2Si_2$ at field-induced QCP indcating change of carrier density

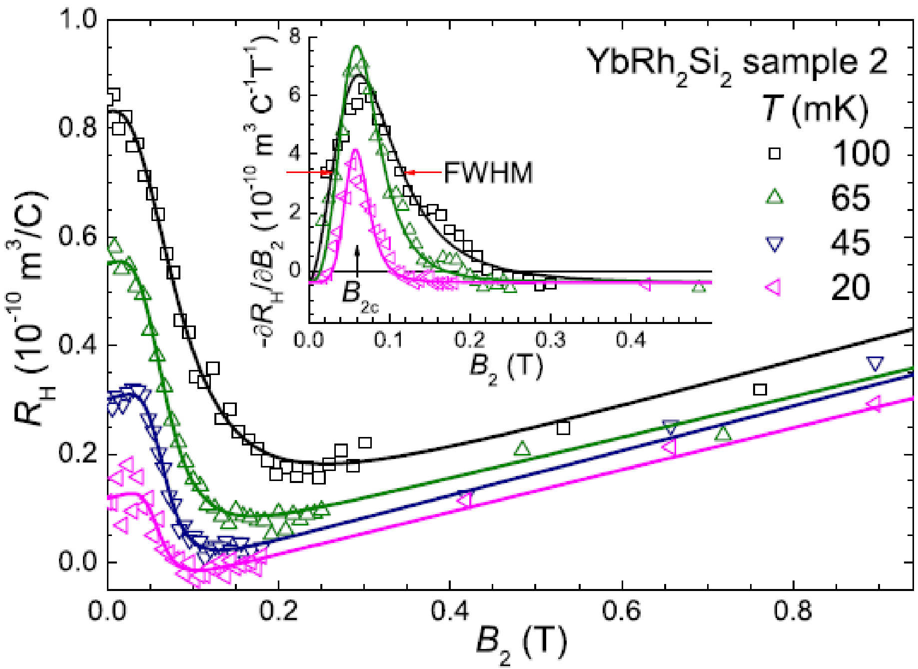

FWHM of carrier-density change goes to zero as $T \to 0$

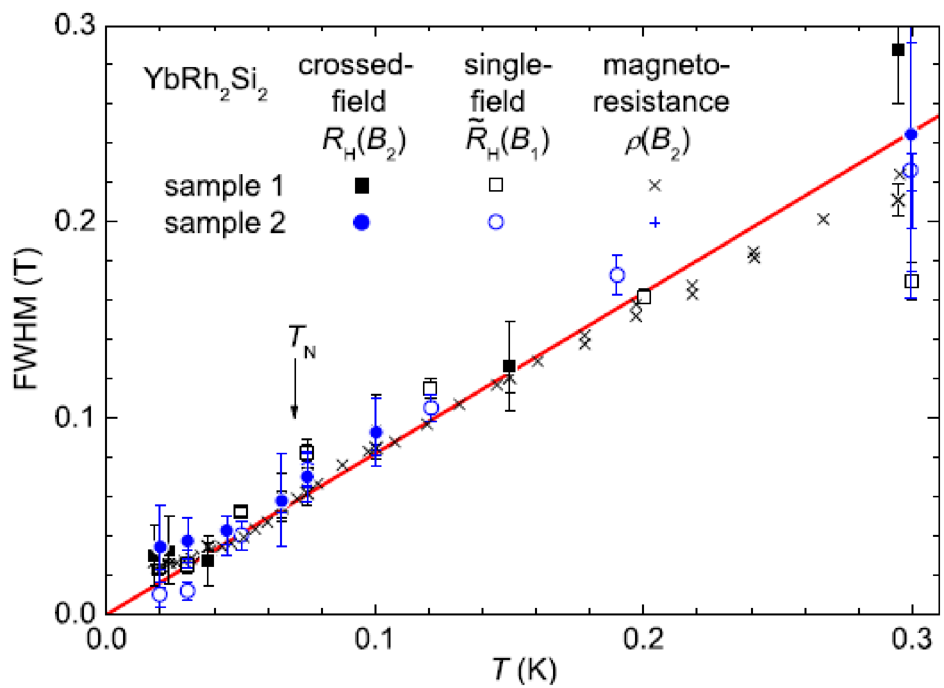

Interpretation: Fermi volume changes from “large“ to “small“ when below B_c magnetic order sets at the magnetic QCP:

4*f* electrons become become localized

“Kondo breakdown“

High-resolution UPS measurements to determine T_K across the quantum critical point

Experiments: M. Klein, A. Nuber, F. Reinert
Theory: J. Kroha
PRL 2008

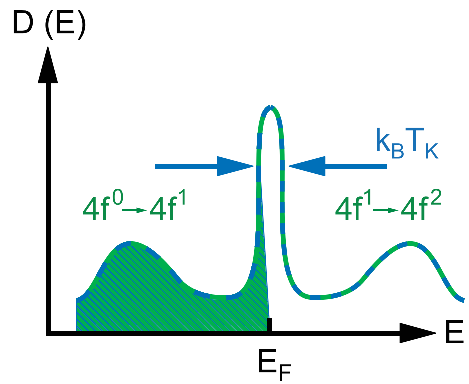

What is the fate of the Kondo resonance?

UPS experiment:

Cleaving $CeCu_{6-x}Au_x$ *in situ* at low T

Photoemission measures occupied states only – some states above E_F are occupied states according to the Fermi-Dirac function $f(E)$

Obtain the DOS for these states by dividing the raw data by $f(E)$

Nearly complete Kondo resonance becomes visible

Local quantum criticality: breakdown of Kondo effect?

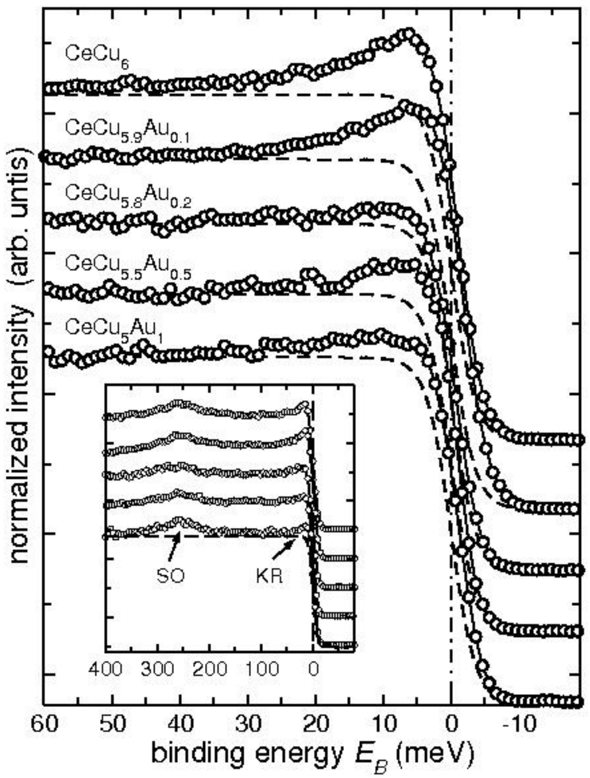

$T > \{T_K, T_{coh}, T_N\}$

High-resolution UPS ($\hbar\omega$ = 40.8 eV)

M. Klein, A. Nuber, F. Reinert

Fits with single-impurity Anderson model/NCA

J. Kroha

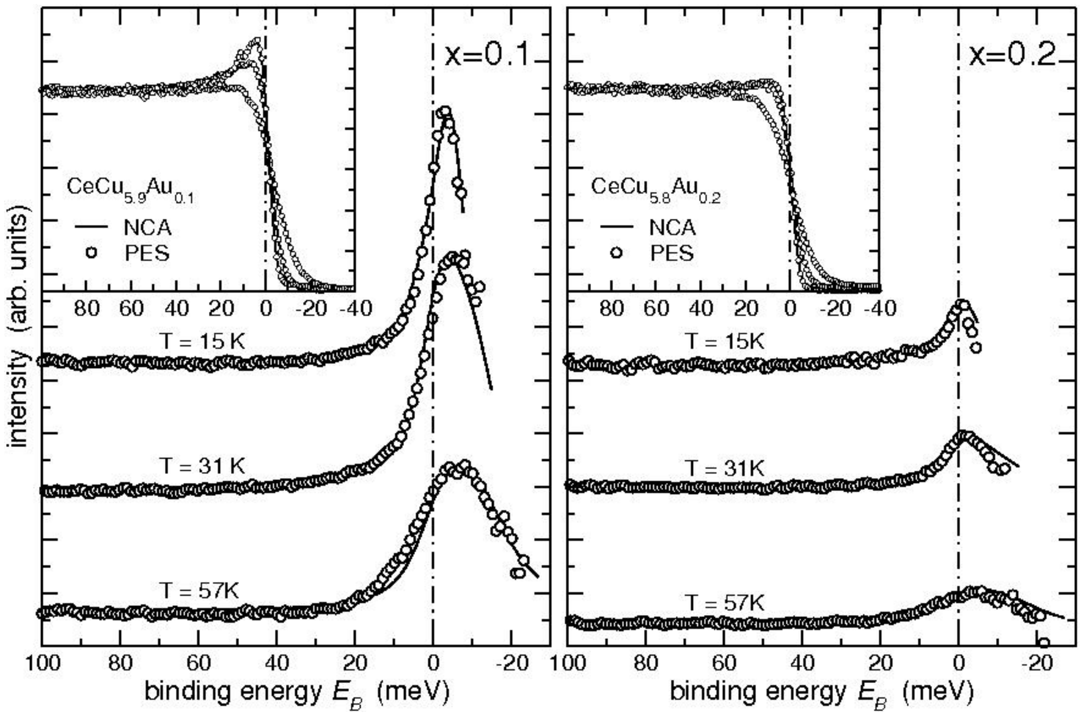

Strong drop of T_K in $CeCu_{6-x}Au_x$ close to x_c

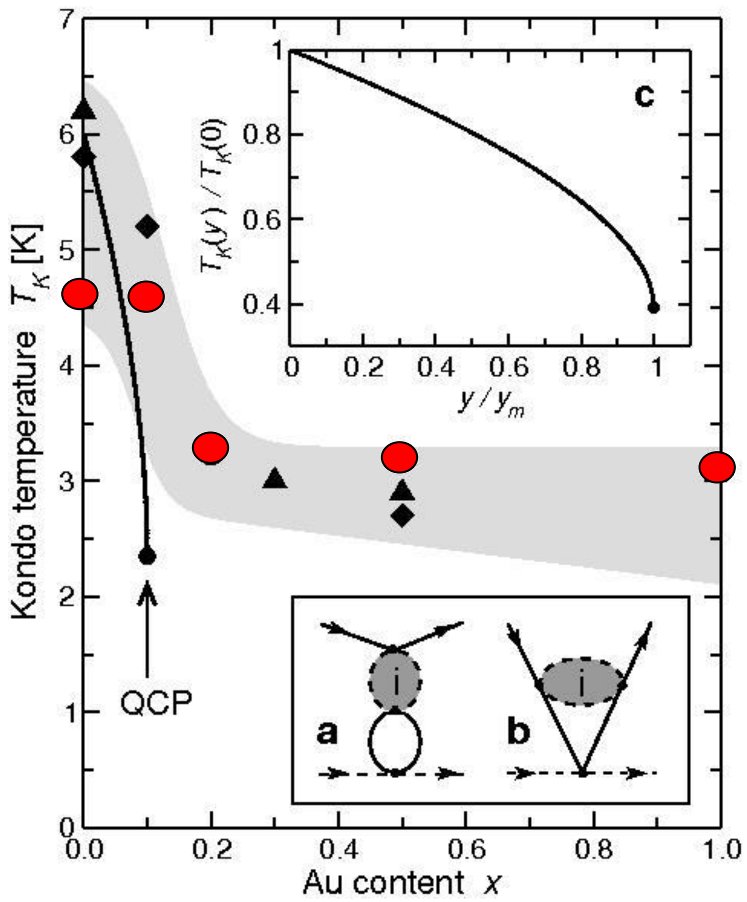

Effective single-impurity model where Kondo exchange J is renormalized by local spin fluctuations at surrounding Kondo ions, neglect of coherence effects

$T_K(y)/T_K(0)$, y is a measure of RKKY interaction, solutions only for $y < y_m$.

J. Kroha

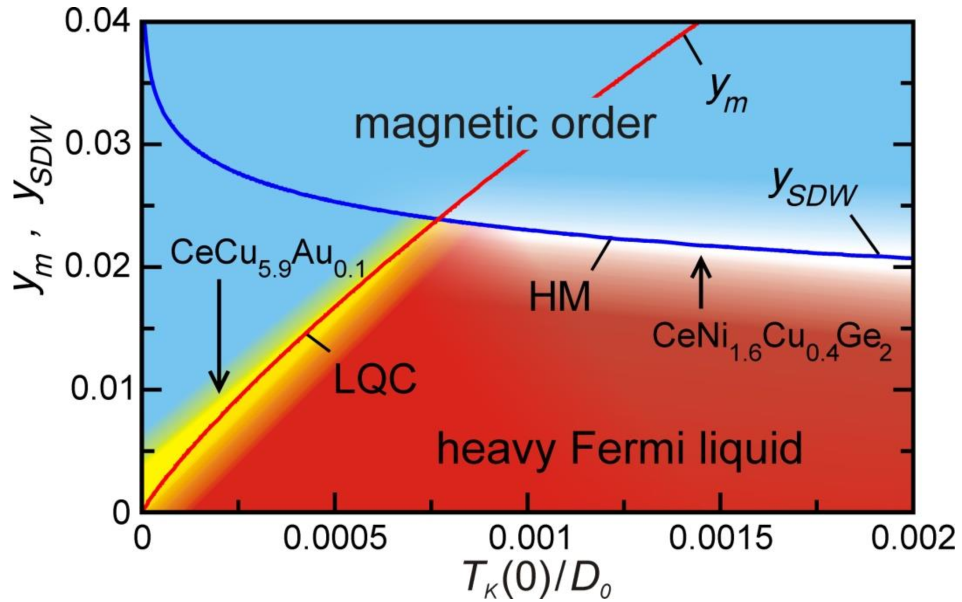

Distinction between Hertz-Millis and Kondo-breakdown (local) scenario ?

cf. $CeRhIn_5$ and $CeCoIn_5$: $T_K \approx 0.1$ and ≈ 1 K

J. D. Thompson

Different scenarios for different tuning parameters in $CeCu_{6-x}Au_x$?

Interplay of concentration and pressure tuning

Pressure dependence of T_N

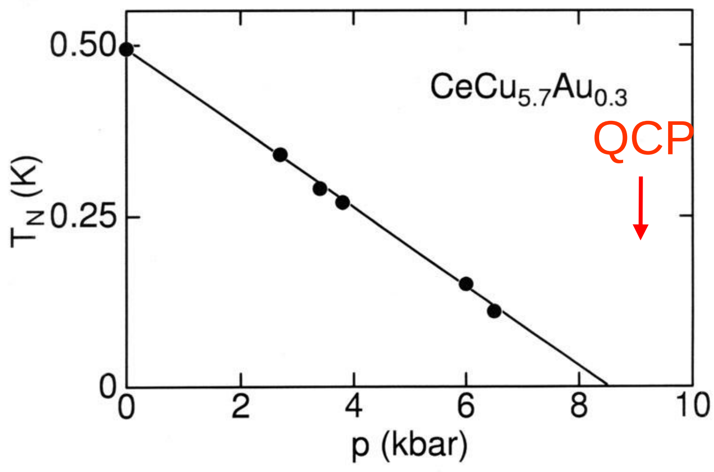

Surprising universality of C/T at quantum critical points

$x = 0.1$	$p = 0$
x = 0.2	$p = 4.1$ kbar
$x = 0.3$	$p = 8.2$ kbar

Suggestive of 2D fluctuations under pressure

Specific heat

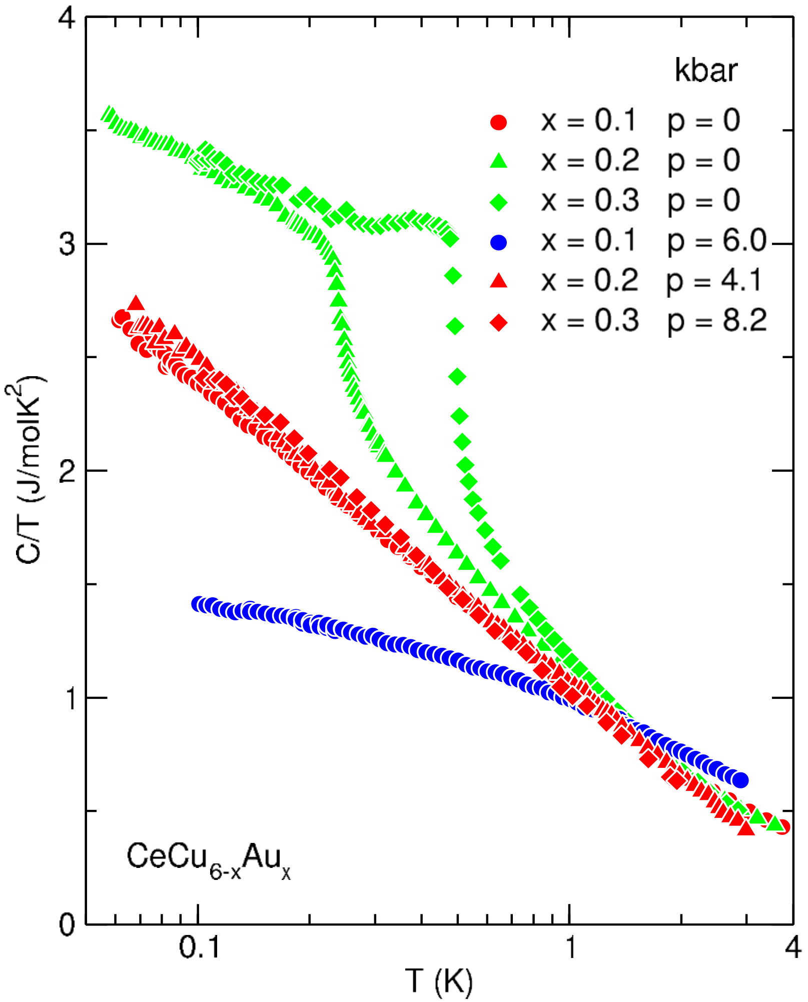

Evolution of the magnetic structure of $CeCu_{5.5}Au_{0.5}$ under hydrostatic pressure

A. Hamann, D. Reznik, O. Stockert, V. Fritsch

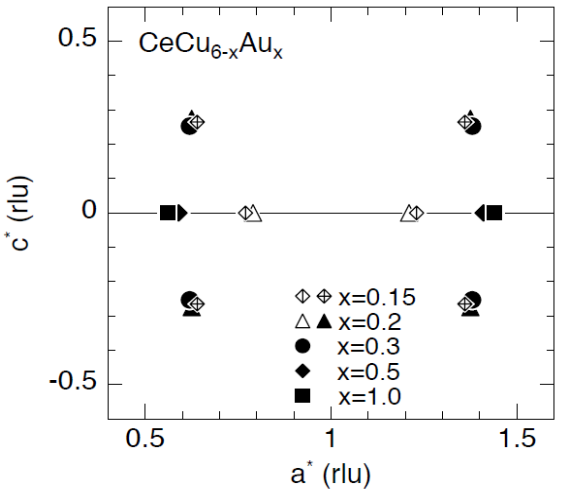

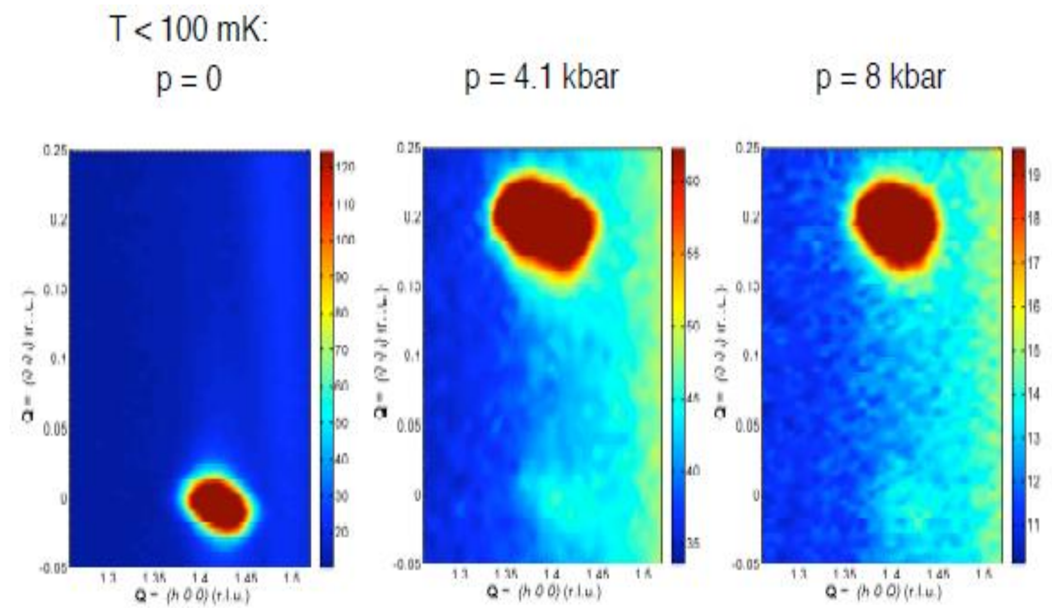

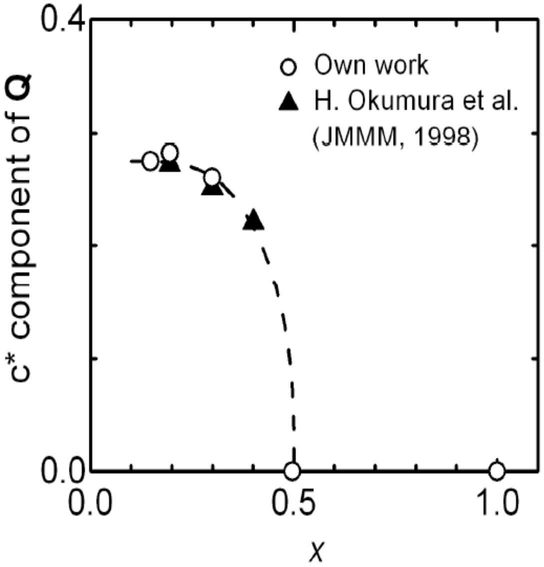

Change of T_N, ordering wave vector, and ordered moment with pressure ($p = 0 \rightarrow 8$ kbar) and Au content ($x = 0.5 \rightarrow 0.3$) is nearly identical!

Strong change of Q is in marked contrast to smooth $T_N(x)$ dependence

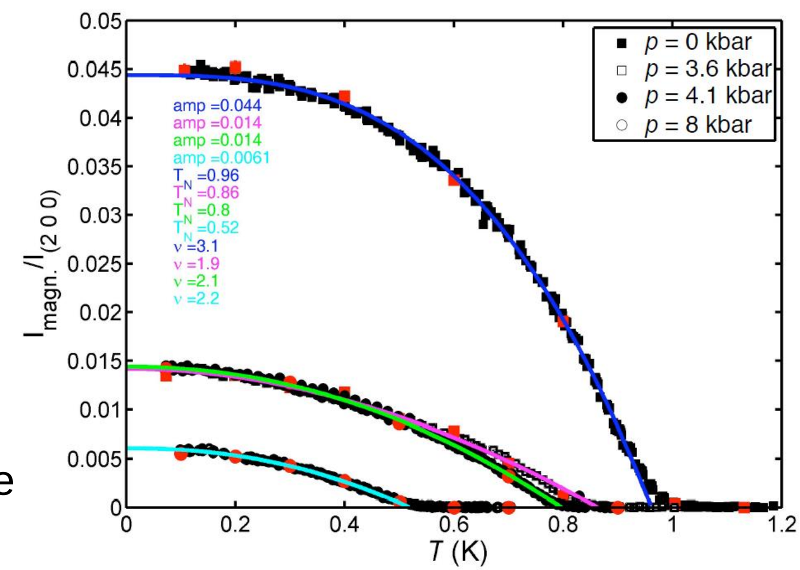

Tuning the magnetic instability of $CeCu_{1-x}Au_x$ (x = 0.2) by pressure or magnetic field: specific heat

at p_c: $C/T \sim \ln(T_o/T)$
2D fluctuations (?)

at B_c: $C/T \sim 1 - a'\sqrt{T}$
standard 3D fluctuations - SRC (?)

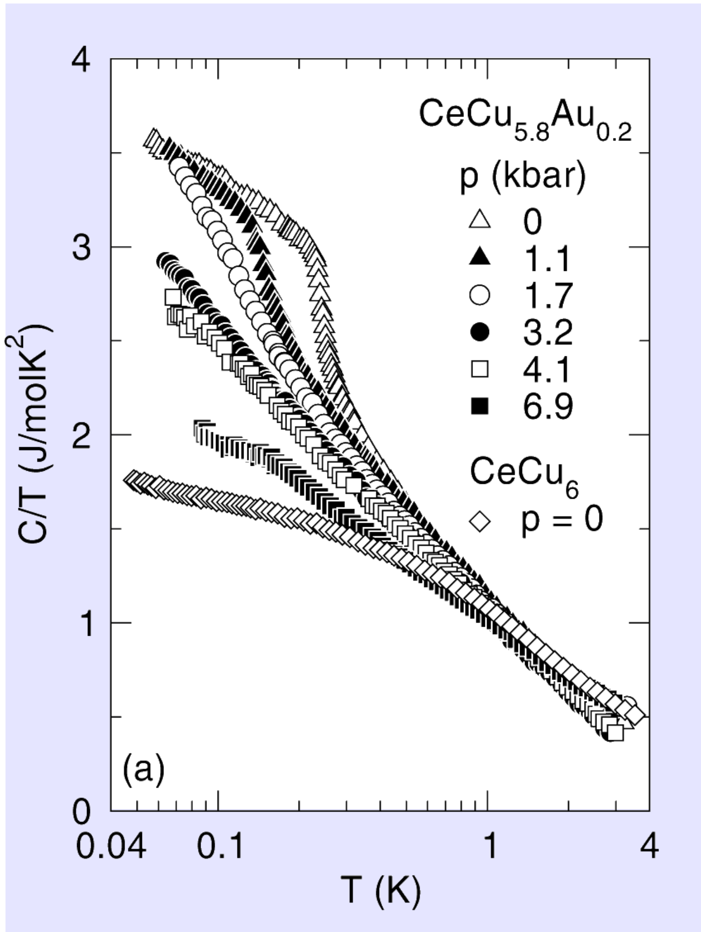

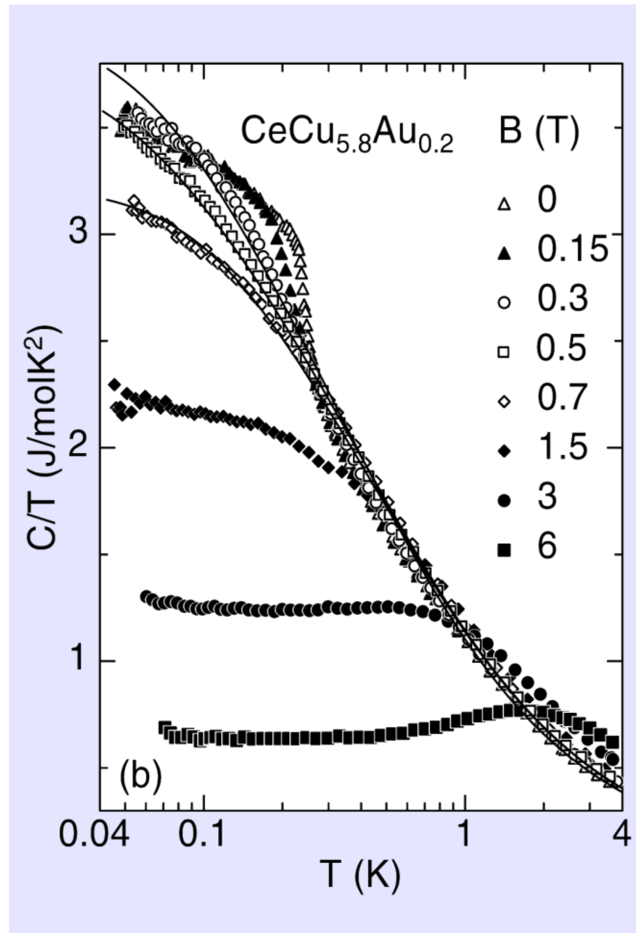

Field dependence of elastic scattering intensity

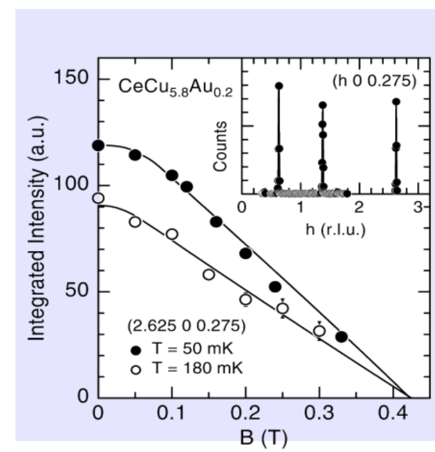

Inelastic neutron scattering at the field-induced instability in $CeCu_{5.8}Au_{0.2}$

Fit of $\chi'' T^{\alpha}$ vs. E/T^{β} with appropriate scaling functions

$\alpha = 1.5$, $\beta = 1.5$ (standard 3D scenario) $\alpha = 0.8$, $\beta = 1$ (as for x = 0.1, B = 0)

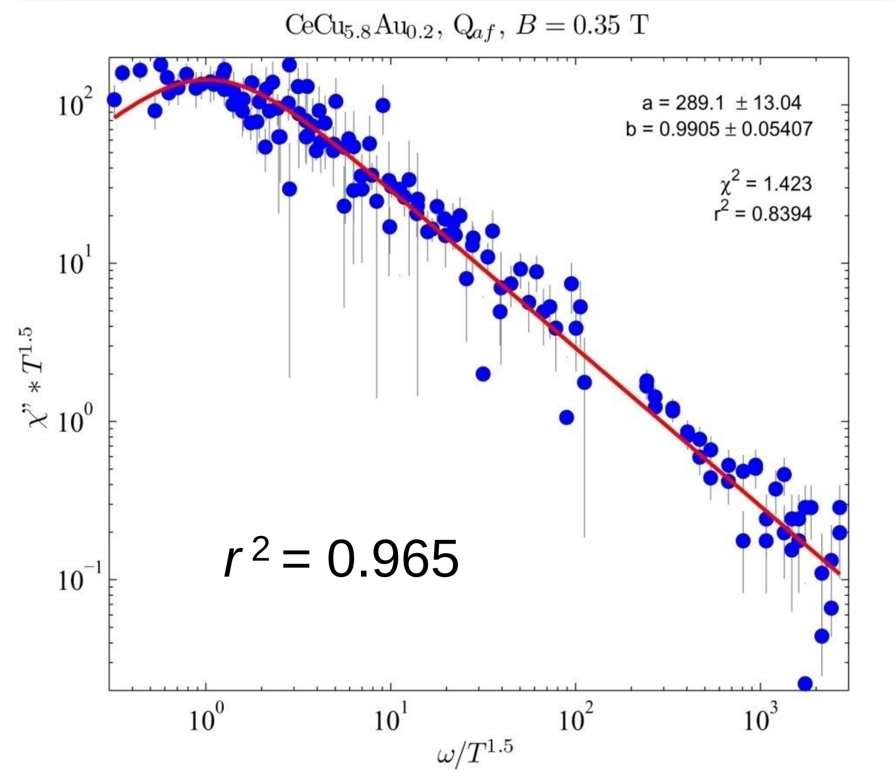

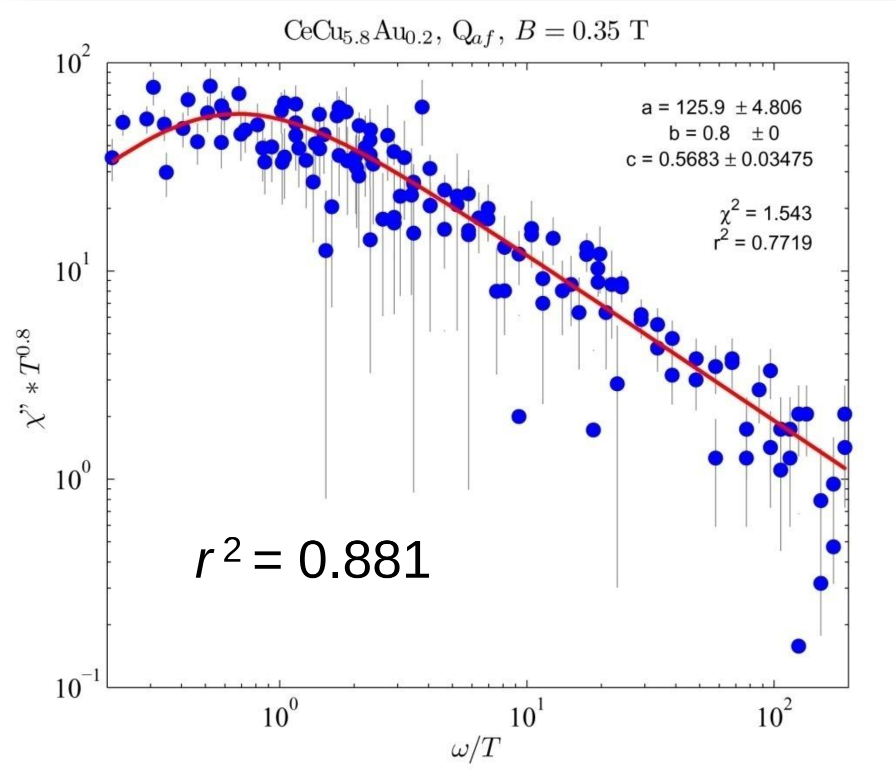

O. Stockert et al., PRL 2007

Possible additional phase line at $T = 0$

LAF: localized-moment magnetic order (large moments)

IAF: Itinerant magnetic order spin-density wave (small moments)

Q. Si et al.
P. Coleman

B: “2D local” QCP

A: 3D itinerant QCP (Hertz-Millis)

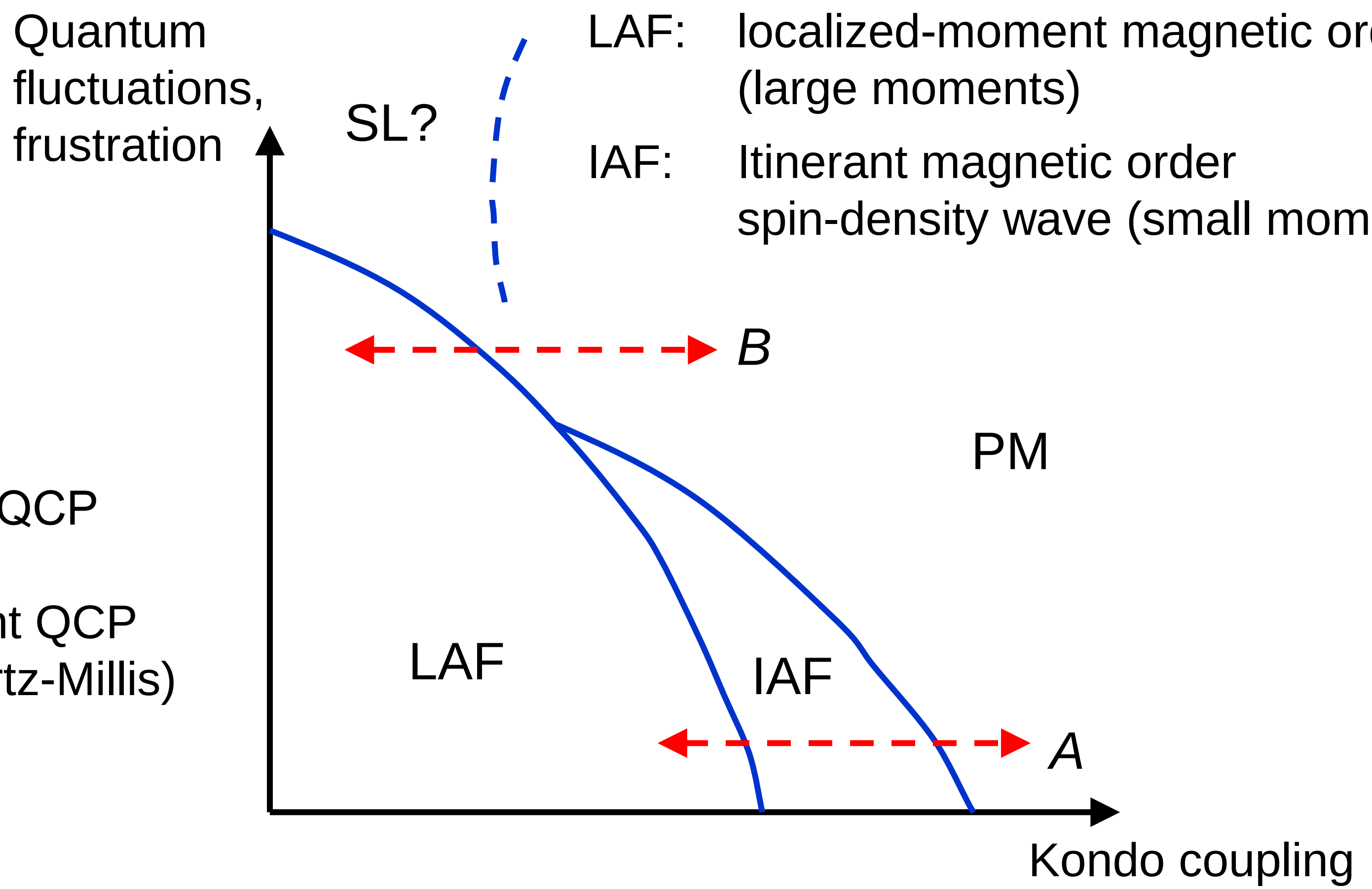

Internal consistency for $CeCu_{6-x}Au_x$
Lowering the effective dimensionality leads to an increase of quantum fluctuations, and thus to the local QCP. Magnetic field restores 3D and hence yields Hertz-Millis

cf. experiments on Co- and Ir-doped $YbRh_2Si_2$ *S. Friedemann et al,, Nature Phys. 2009*

Global phase diagram for quantum-critical heavy-fermion systems

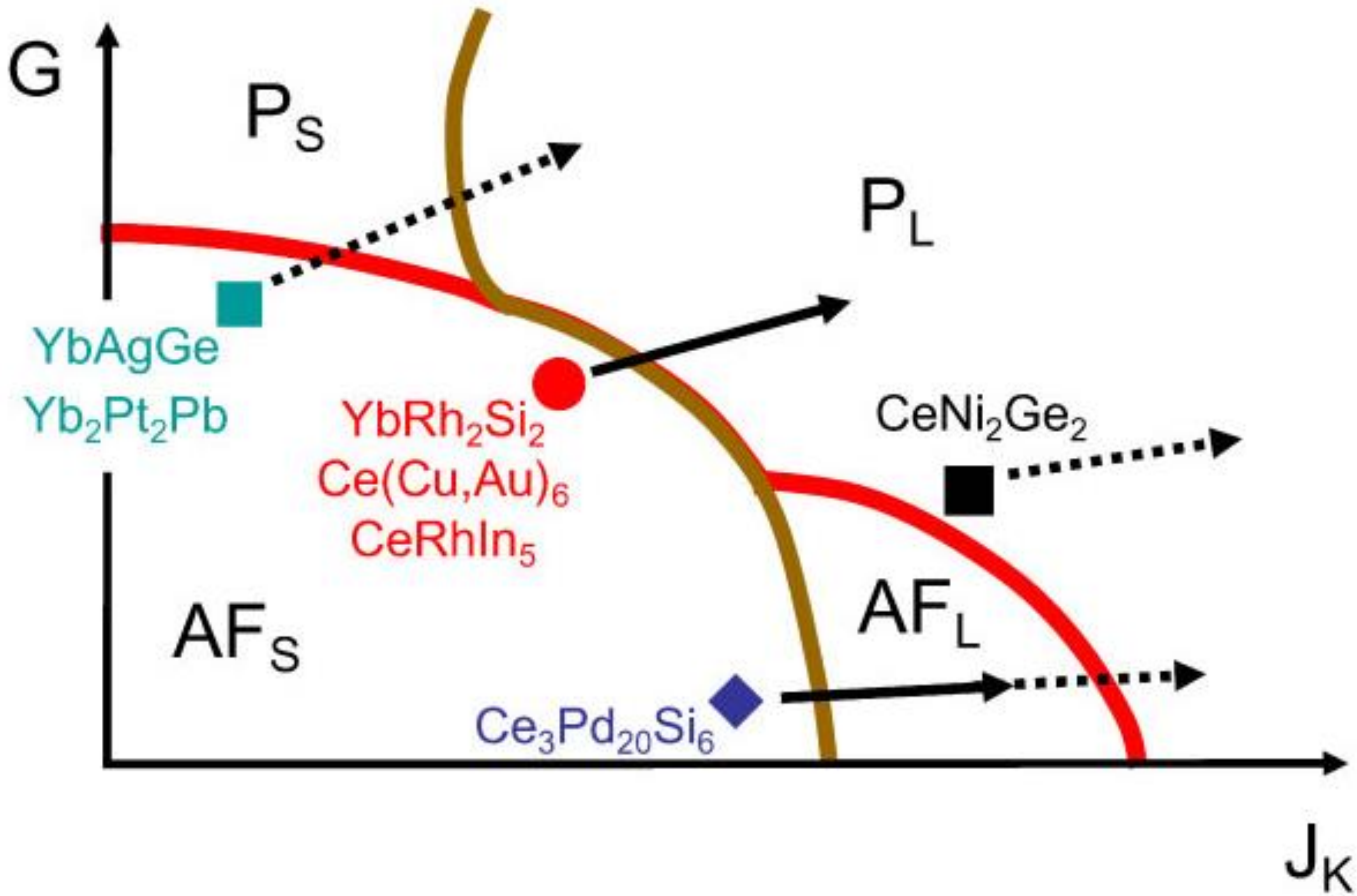

*Q. Si, Physica B **378–380,** 23 (2006)*

*Q. Si and S. Paschen, Phys. Status Solidi B **250**, 425 (2013)*

Possible continuous evolution from local-moment to itinerant antiferromagnetism in Kondo systems

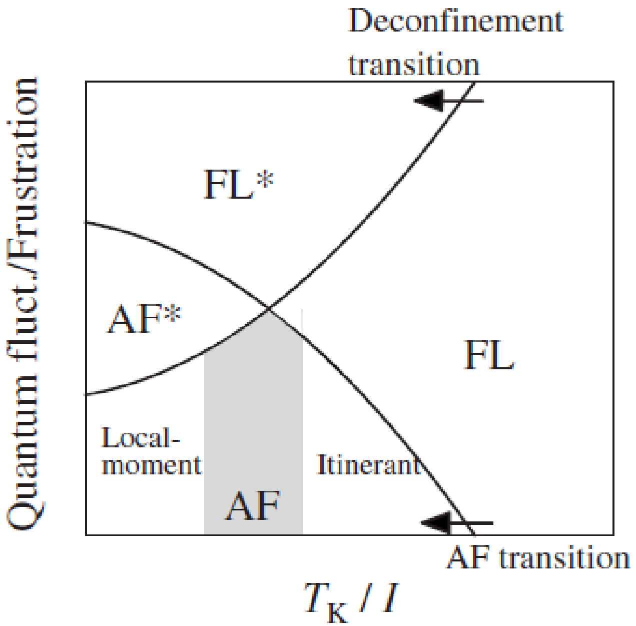

M. Vojta, PRB 78, 125109 (2008)
See also T. Senthil et al., PRL 90, 216403 (2003)

LAF - IAF transition may be gradual

How can one experimentally "control" of the vertical axis?

What is the effect of magnetic field in this plot?

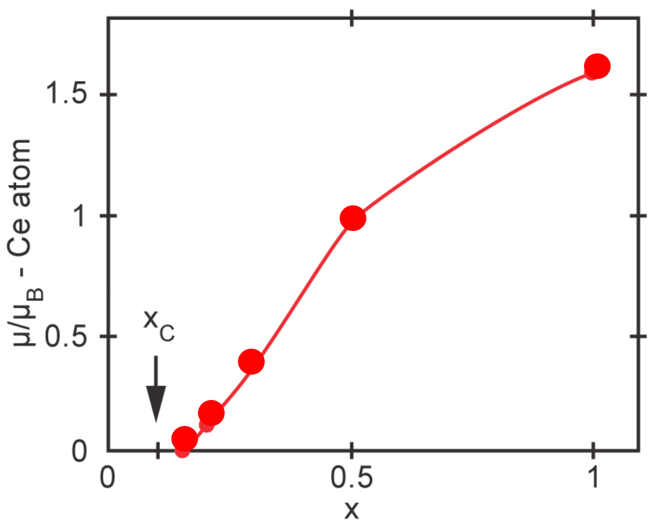

$CeCu_{1-x}Au_x$: gradual evolution of ordered magnetic moments (from ENS)

Tiny specific-heat anomaly at T_N on top of a large "non-Fermi-liquid" background

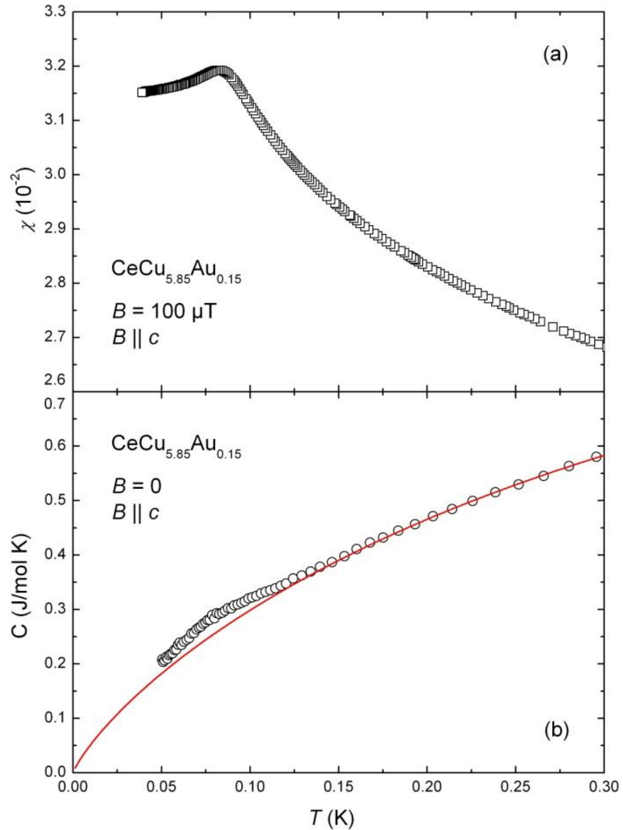

Scenarios for quantum criticality in heavy-fermion systems

conventional

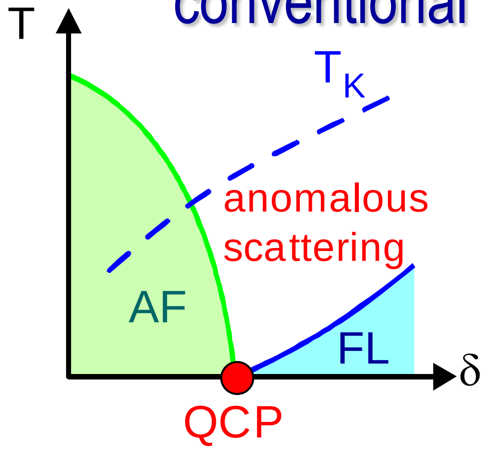

Scattering of heavy quasiparticles
by spin fluctuations:
diverging *m** for 3D FM and 2D AF

unconventional

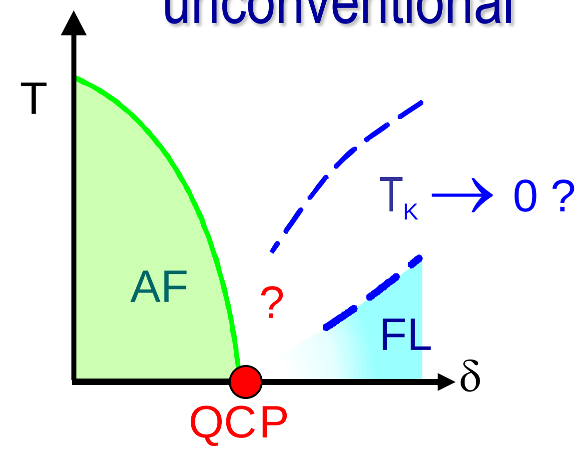

Unbinding of composite
heavy quasiparticles;
local quantum criticality

$CeCu_2Si_2$ | $Ce_{1-x}La_xRu_2Si_2$ | $CeNi_2Ge_2$

$CePd_2Si_2$ | $UCu_{5-x}Pd_x$ | $CeCu_{6-x}Au_x$ | $YbRh_2Si_2$

Critical quasiparticles

Abrahams, Wölfle, Schmalian

Fractionalized Fermi liquids

Senthil, Sachdev, Vojta

Change of Fermi volume ?
Dimensionality ?
Disorder effects ?

Hertz, Millis, Moriya, Rosch et al.

Coleman, Si, Pepin et al.

Anomalous quantum criticality in $CeCu_{6-x}Au_x$ described in terms of critical quasiparticles

*Wölfle, Abrahams, PRB **84**, 041101 (2011)*
*Abrahams, Wölfle, PNAS **109**, 3218 (2012)*
*Abrahams, Schmalian, Wölfle, PRB **90**, 045105 (2014)*

Quasiparticle weight factor Z at E_F given by

$Z^{-1} = 1 - \partial \mathrm{Re}\Sigma(\omega)/\partial\omega = m^*/m$

Non-Fermi liquid: $Z = 0$.

Allow for $Z = Z(\omega) \sim \omega^{\eta}$,
with $Z = 0$ at E_F

Predictions for
2D quantum fluctuations

Specific heat
$C/T \sim T^{-1/8}$

Thermal expansion
$\alpha_V/T \sim T^{-1}$

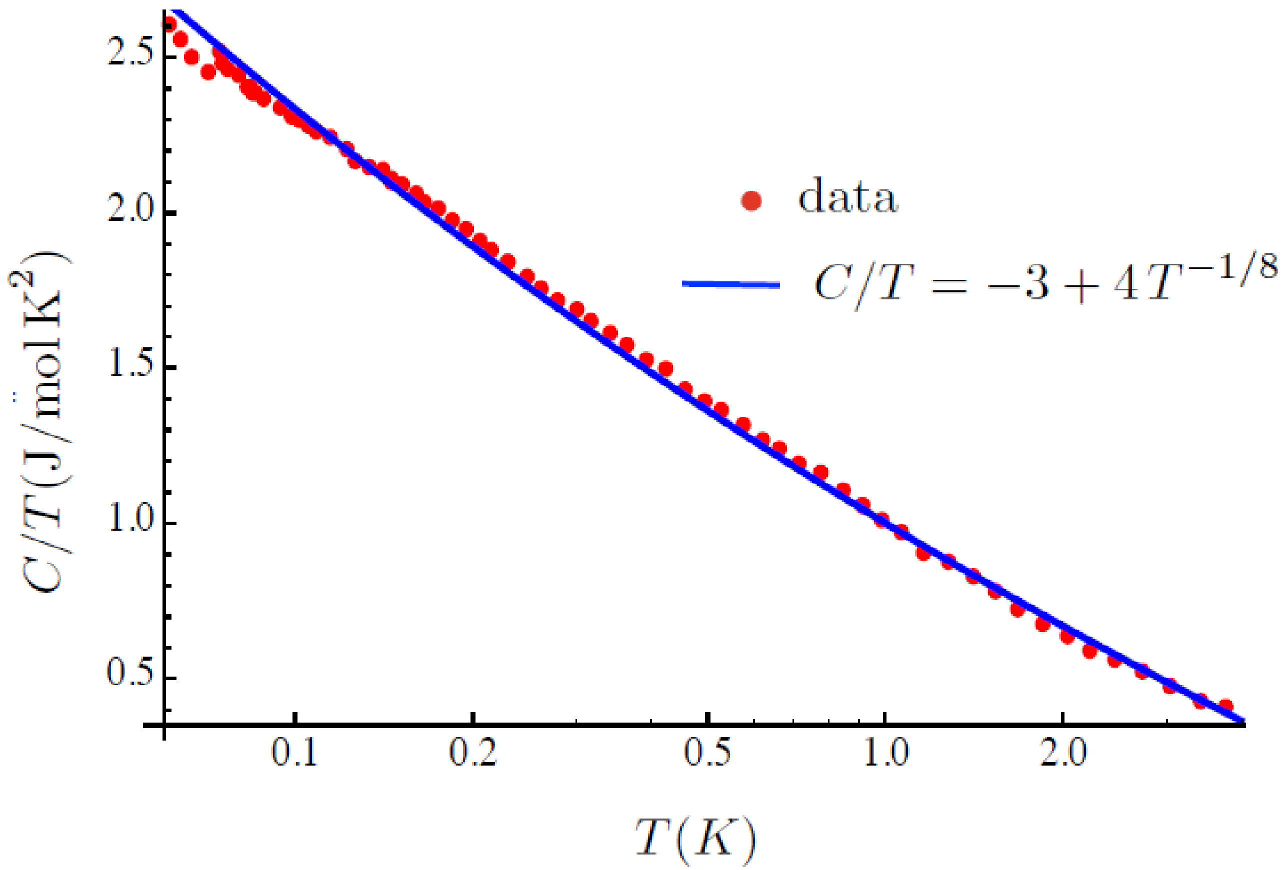

Thermal expansion – a sensitive thermodynamic probe of quantum criticality

Volume thermal expansion of $CeCu_{6-x}Au_x$

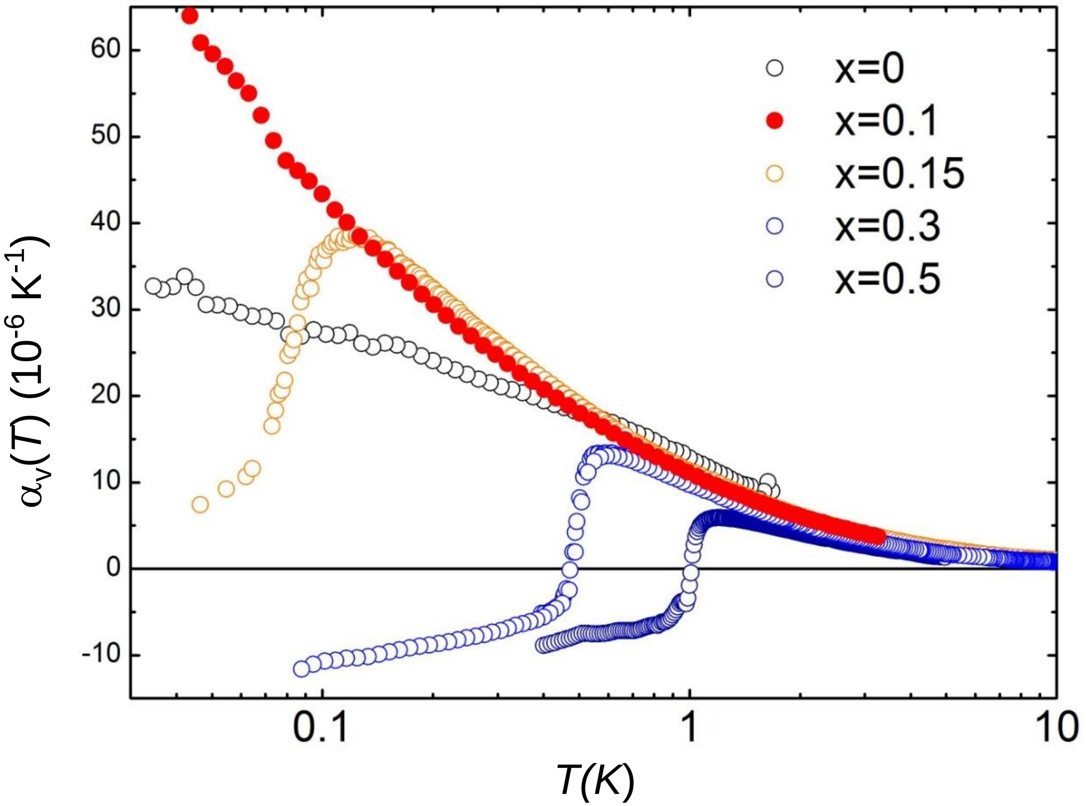

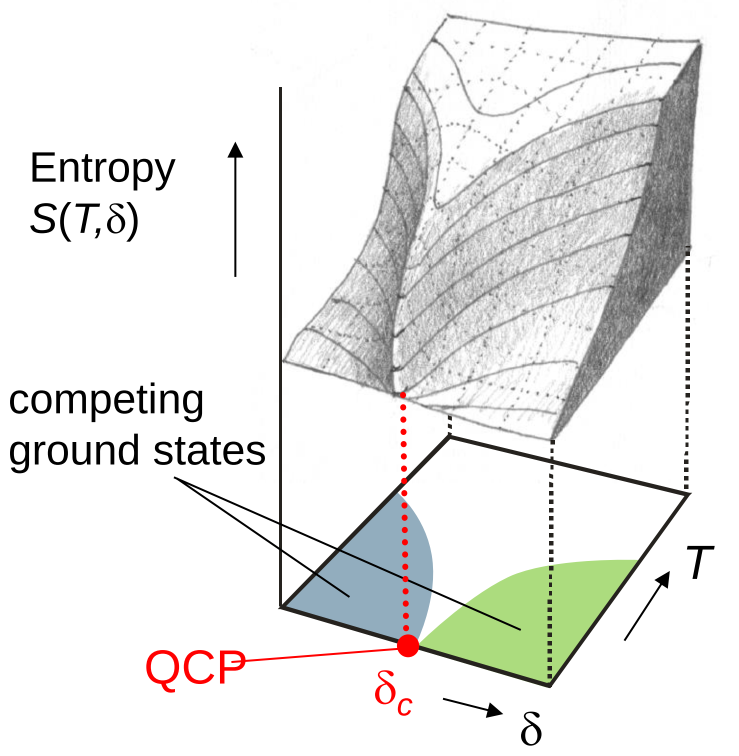

Sign change at the magnetic transition because $\alpha_v = dV/dT = - dS/dp$

Divergence for $T_c \rightarrow 0$

Theory: Zhou, Si, Garst, and Rosch, PRL 2002

Thermal expansion as a sensitive probe of phase transitions approaching a QCP: example $CeCu_{5.85}Au_{0.15}$

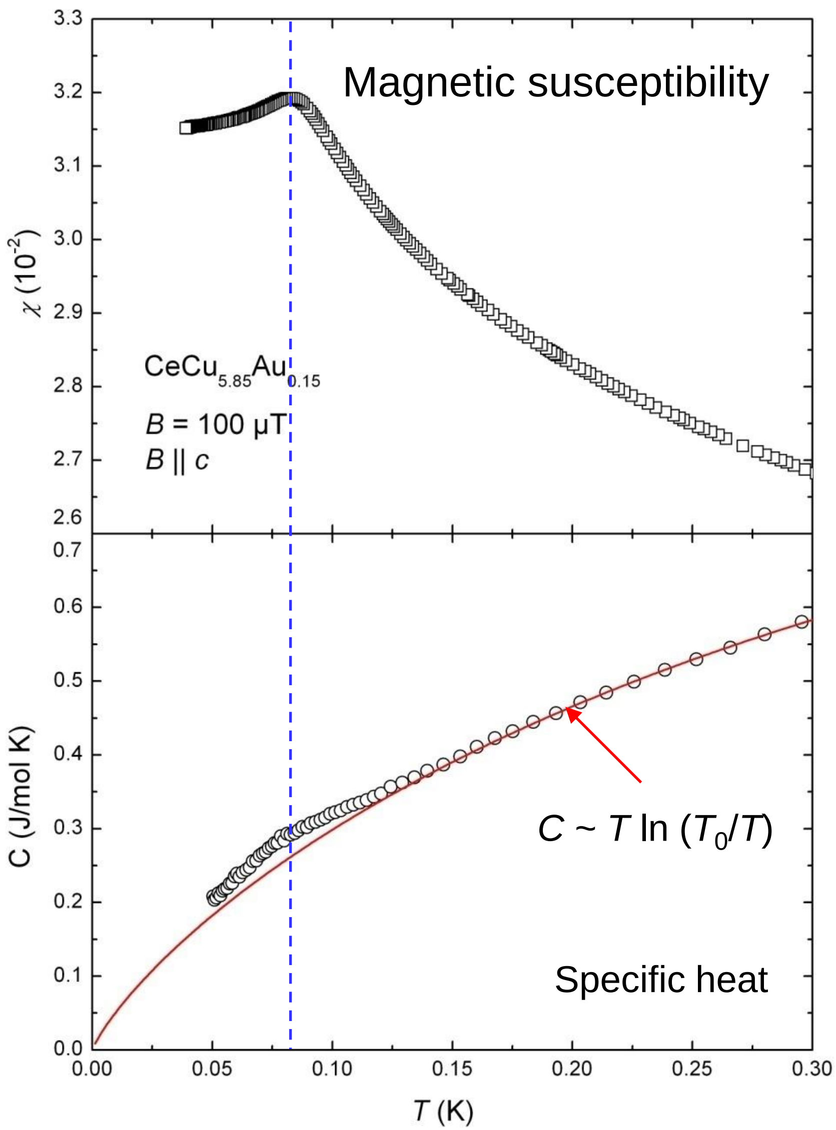

Antiferromagnetic order below T_N = 82 mK

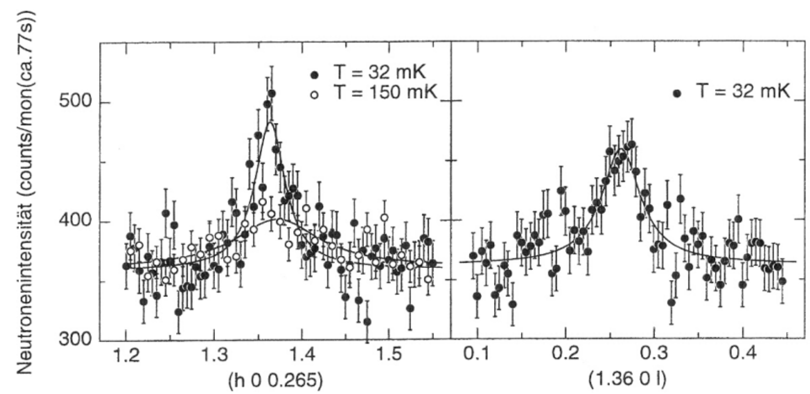

tiny specific-heat feature at T_N in excess of NFL $C \sim T \ln (T_0/T)$, very small ordered moment, large thermal expansion

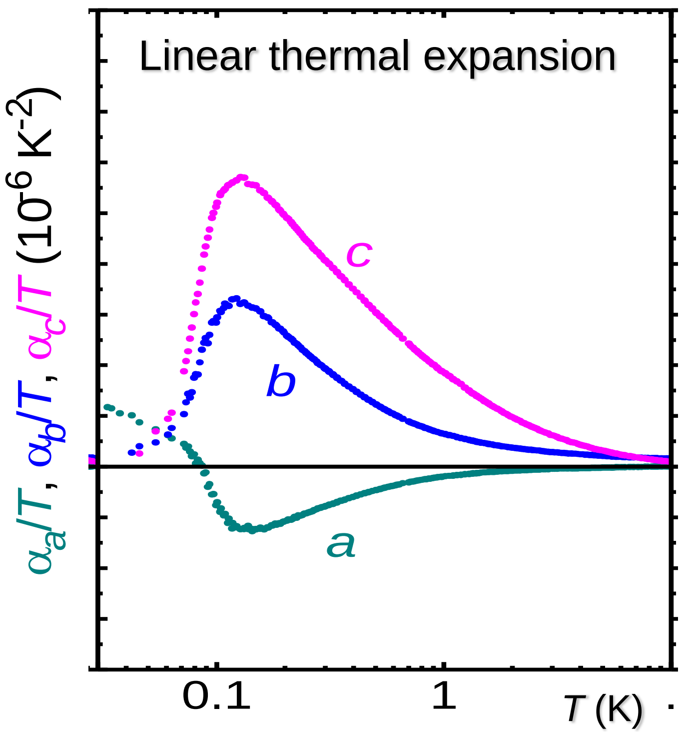

Theory: Zhu et al., PRL 2003

Thermal expansion close to a QCP

Fermi liquid at low *T*

$$\frac{C}{T} = \frac{\partial S}{\partial T} = \gamma = \text{constant.}$$

$$S = \gamma T \;\Rightarrow\; \frac{\alpha_i}{T} = -\frac{1}{VT}\frac{\partial S}{\partial \sigma_i} = -\frac{1}{V}\frac{\partial \gamma}{\partial \sigma_i} = \text{constant.}$$

Grüneisen ratio

$$\Gamma_i = \frac{\alpha_i}{C} = \text{const}$$

Deviation from Fermi-liquid behavior at a QCP

*Zhu, Garst, Si, and Rosch, PRL **91**, 066404 (2003)*

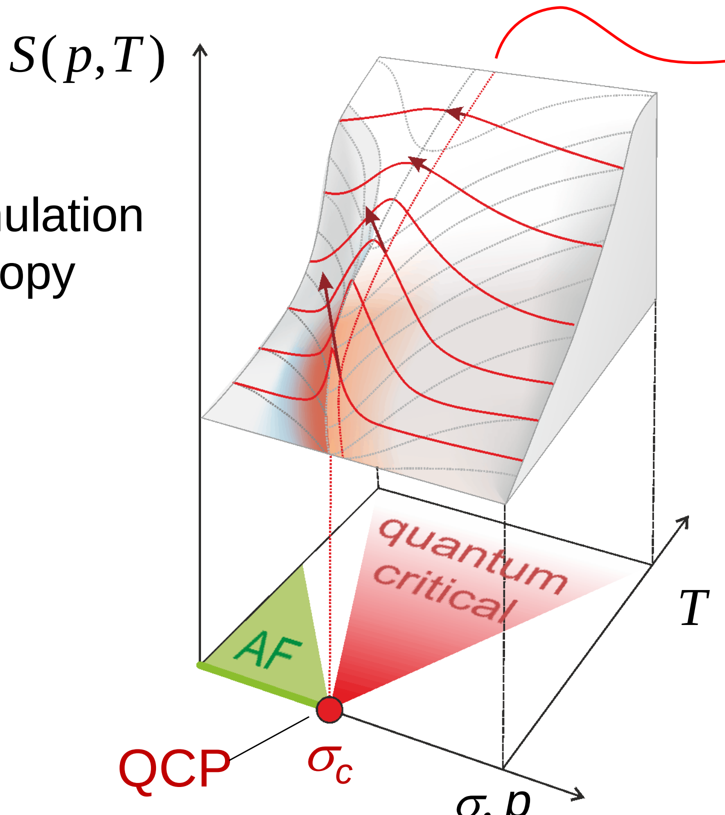

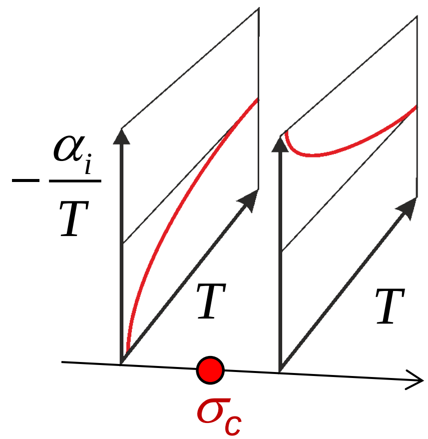

sign change at σ_c

divergence of Γ_i

$$E^* \to 0:\; \Gamma_i = \frac{1}{E^*}\frac{\partial E^*}{\partial \sigma_i} \to \infty$$

Divergence of the volume Grüneisen parameter for T → 0 at a quantum critical point

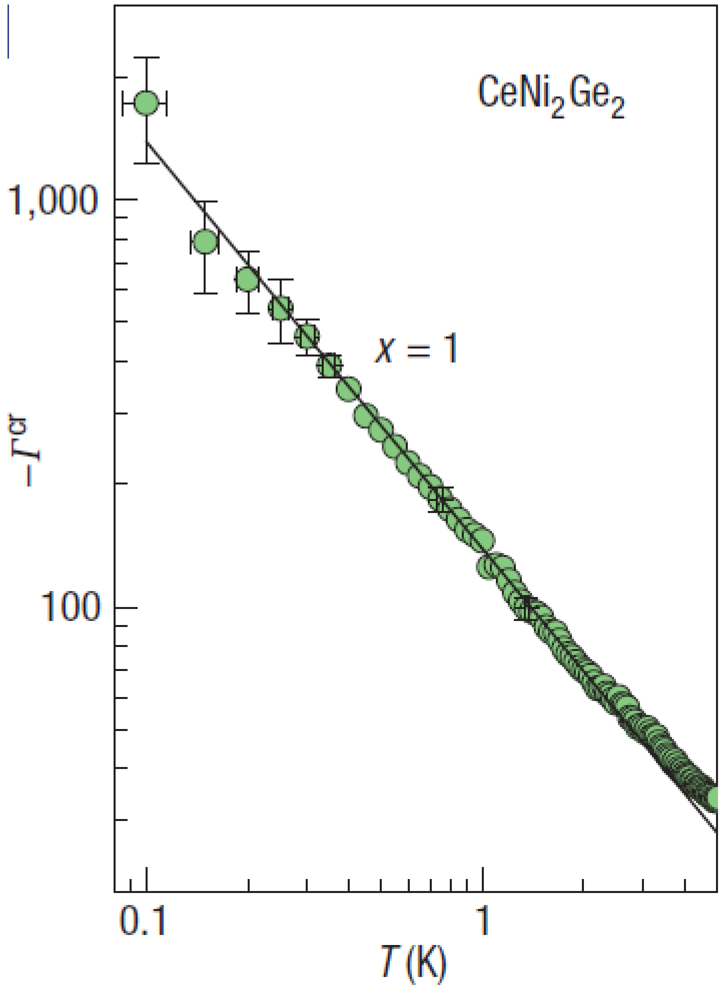

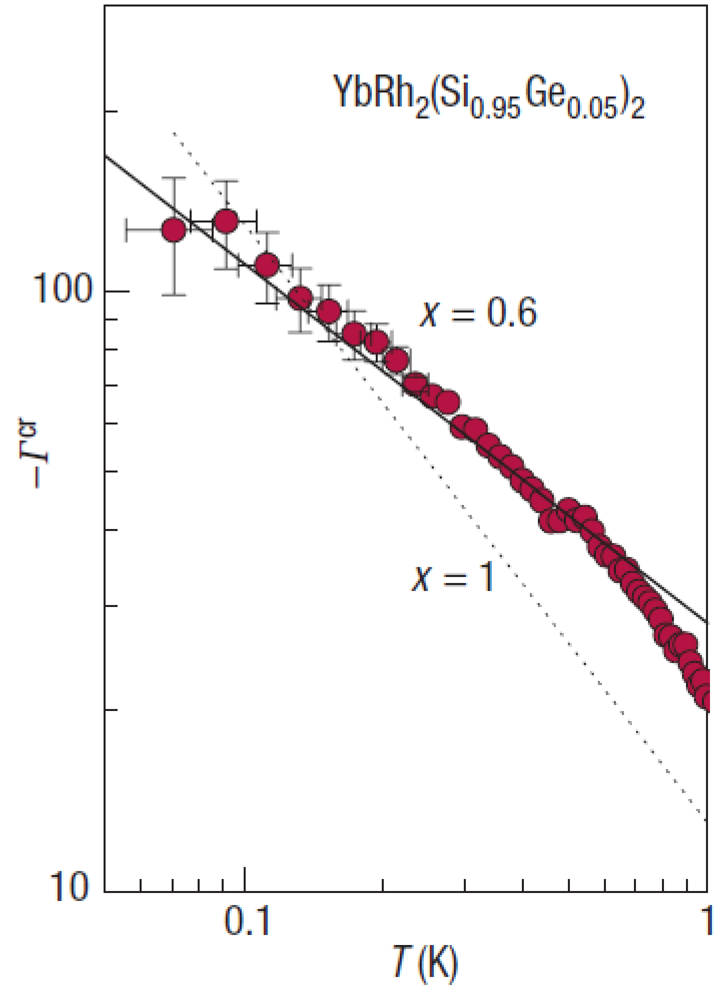

*Prediction: Zhu, Garst, Si, and Rosch, PRL **91**, 066404 (2003)*
*Experiments: Küchler et al., PRL **91**, 066405 (2003); PRL **93**, 096402 (2004)*

Thermal expansion as a sensitive probe of phase transitions approaching a QCP: example $CeCu_{5.85}Au_{0.15}$

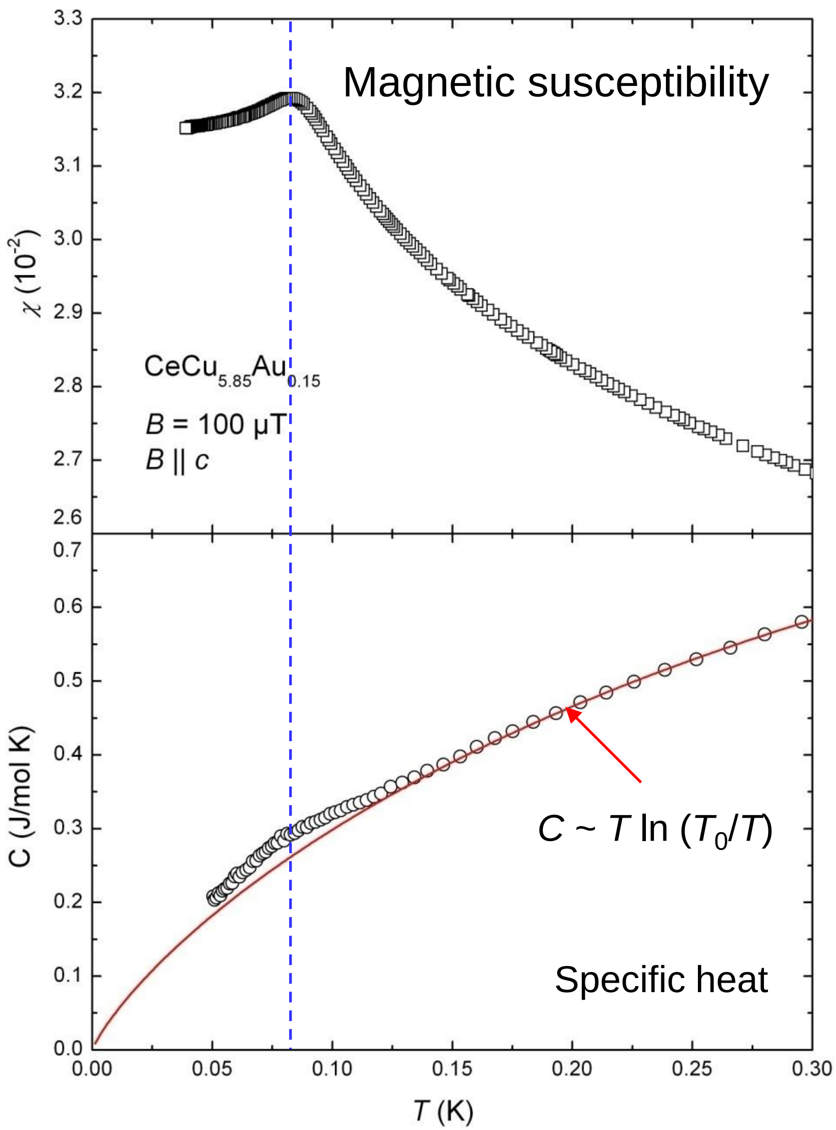

Antiferromagnetic order below T_N = 82 mK

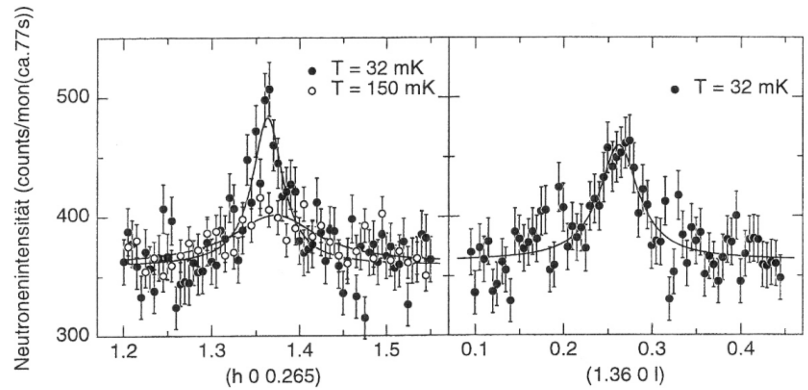

tiny specific-heat feature at T_N in excess of NFL $C \sim T \ln (T_0/T)$, very small ordered moment, large thermal expansion

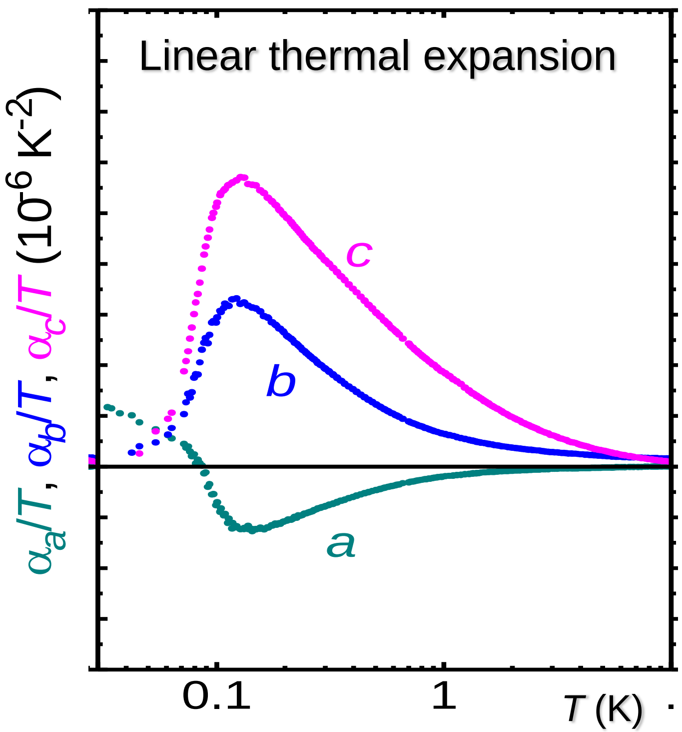

Determining the entropy landscape near quantum criticality

Anisotropic response of thermal expansion to different transitions or excitations in $CeCu_{5.9}Au_{0.1}$

Thermal expansion coefficients α_i (*i = a, b, c)*

$$\alpha_i = \partial\epsilon_i/\partial T = -V^{-1}\partial S/\partial\sigma_i.$$

ε_i and σ_i: strain and stess components
along principal axes
(for orthorhomic or higher symmetry)

T_s:
Small monoclinic distortion of the *ab* plane
($\Theta < 2°$, neglected in the following)

CEF:
thermal excitation to higher CEF doublets – anisotropy reflects the different spatial dependence of CEF wave functions

Low *T*:
passing the coherent Fermi-liquid regime toward a quantum critical point

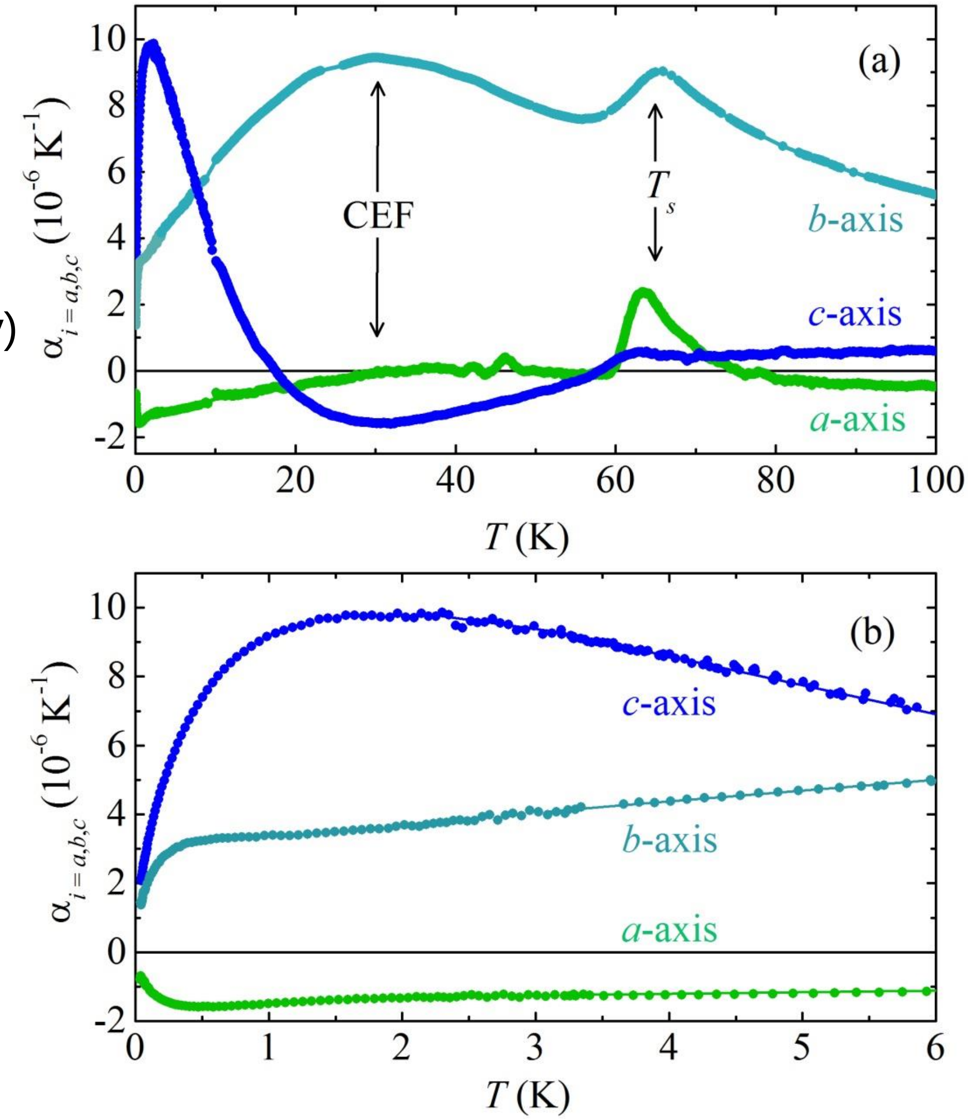

Linear and volume thermal expansivities divided by T for $T \to 0$

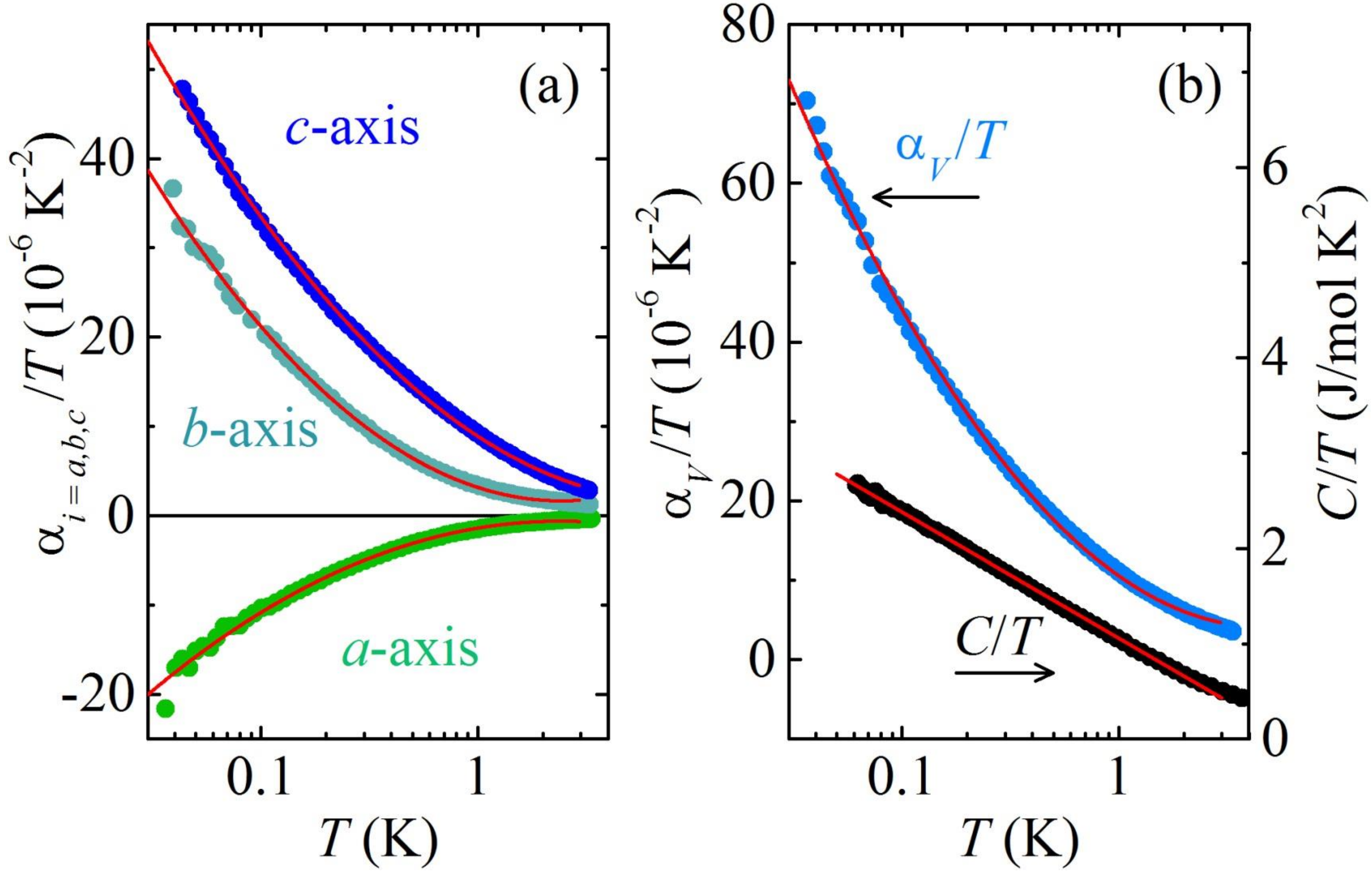

Divergence of $\alpha_V(T)/T$ is stronger than that of C/T ~ $\ln(T_0/T)$, compatible with $\alpha_V(T)/T$ ~ $\ln^2(T_0/T)$

Linear and volume Grüneisen ratios $\Gamma_i = \alpha_i/C$ and $\Gamma_V = \alpha_V/C$

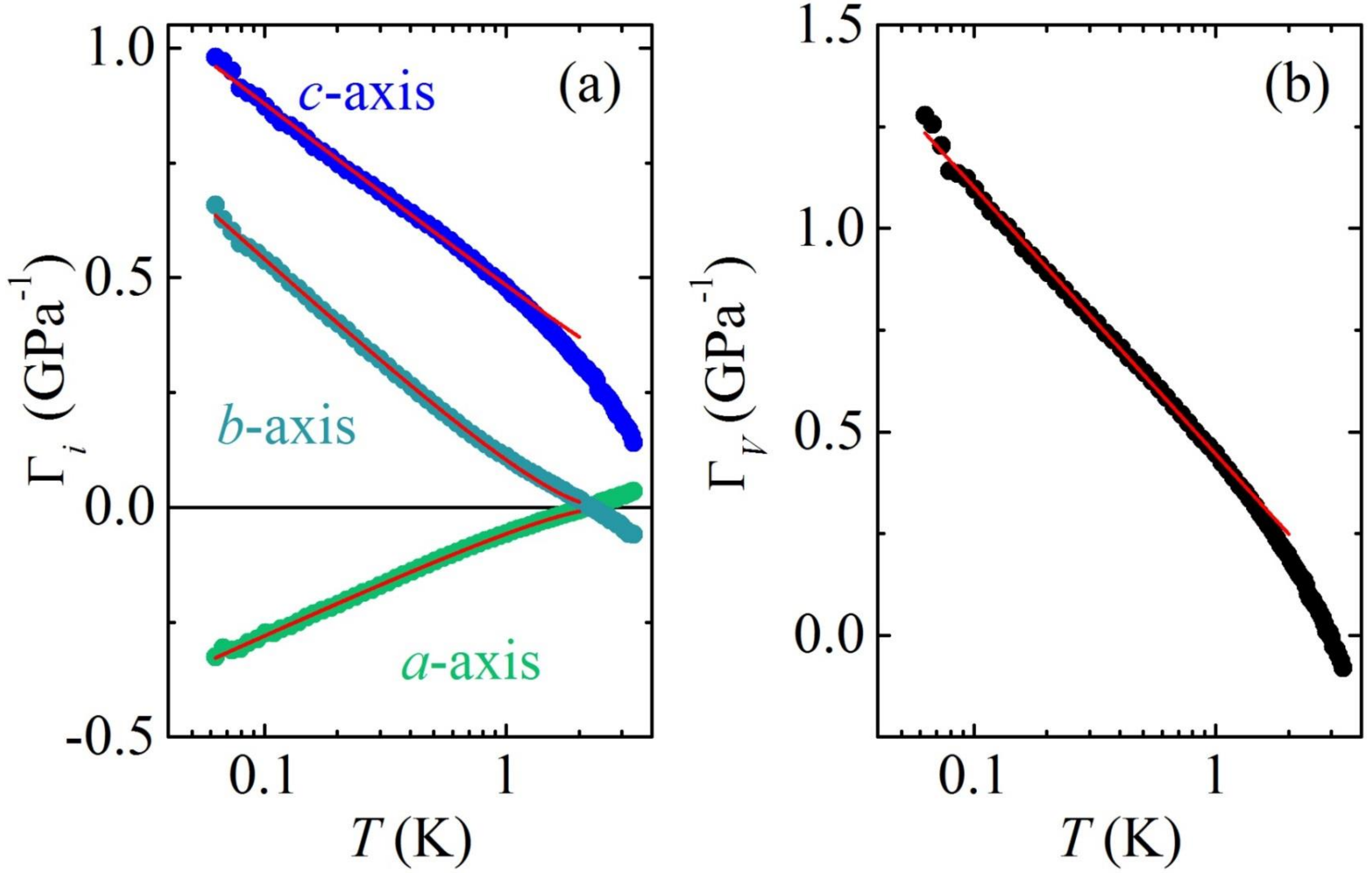

Roughly logarithmic increase toward low T

compatible with local quantum critical scenario (Q. Si et al.)

fit parameters T_{0i} depend on i

Dependence of entropy on arbitrary stress direction

Stress and expansivity tensors

$$\alpha_{ij} = \frac{1}{V}\frac{\partial^2 G}{\partial T \partial \sigma_{ij}} = -\frac{1}{V}\frac{\partial S}{\partial \sigma_{ij}}.$$

(a)

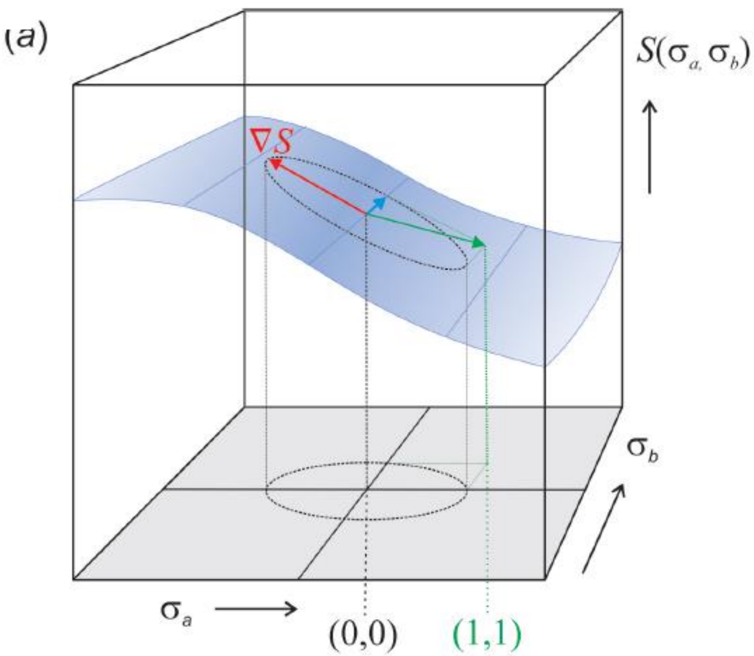

$\sigma_{(lm)}$ picks up the anisotropy:

$\sigma_{(lm)} = 0$ for isotropic systems

For systems with orthogonal or higher symmetry:

$$\frac{\partial S}{\partial \sigma_u} = \vec{\nabla} S \hat{u} = \sum_{i=1}^{3} \frac{\partial S}{\partial \sigma_i} \hat{u}_i = -V \sum_{i=1}^{3} \alpha_i \hat{u}_i.$$

Specific stress combinations:

hydrostatic pressure $\vec{p} = p \times (1, 1, 1).$

stress $\perp$ $\vec{p}$: “pure shear stress“

$$\vec{\sigma}_{(lm)} = \vec{\sigma}_l - \vec{\sigma}_m \text{ with } \vec{\sigma}_l \cdot \vec{\sigma}_m = 0$$

hydrostatic pressure:
volume change
without distortion
(if bulk modulus isotropic)

pure shear stress:
distortion
without volume change

$\sigma_i = \sigma_j$

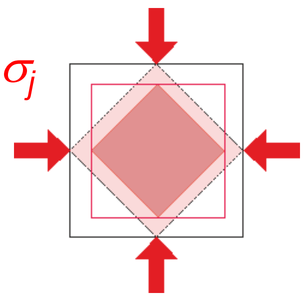

$\sigma_i = -\sigma_j$

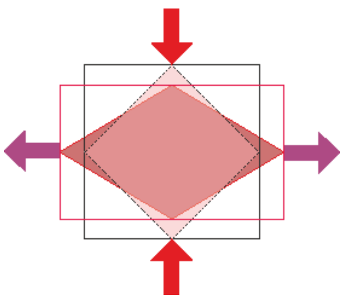

Dependence of entropy on arbitrary stress direction

Stress and expansivity tensors

$$\alpha_{ij} = \frac{1}{V}\frac{\partial^2 G}{\partial T \partial \sigma_{ij}} = -\frac{1}{V}\frac{\partial S}{\partial \sigma_{ij}}.$$

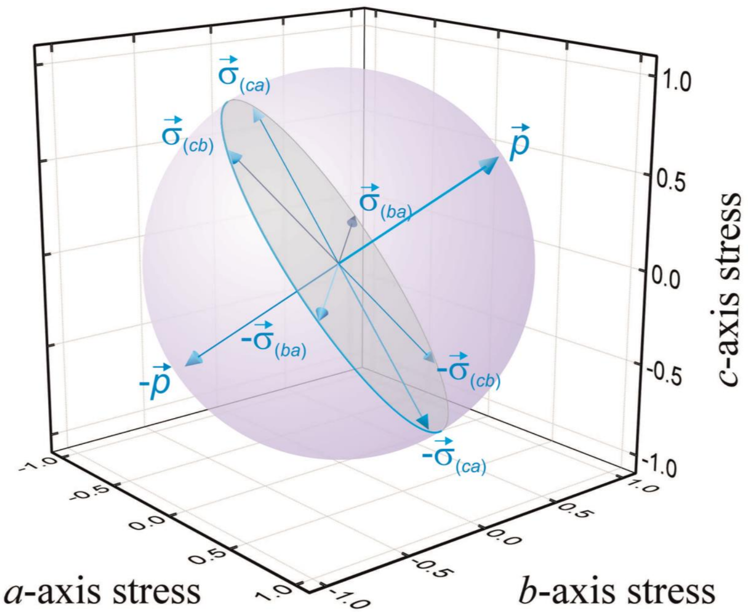

$\sigma_{(lm)}$ picks up the anisotropy:

$\sigma_{(lm)}$ = 0 for isotropic systems

For systems with orthogonal or higher symmetry:

$$\frac{\partial S}{\partial \sigma_u} = \vec{\nabla} S \hat{u} = \sum_{i=1}^{3} \frac{\partial S}{\partial \sigma_i} \hat{u}_i = -V \sum_{i=1}^{3} \alpha_i \hat{u}_i.$$

Specific stress combinations:

hydrostatic pressure $\vec{p} = p \times (1, 1, 1).$

stress $\perp$ $\vec{p}$: “pure shear stress“

$$\vec{\sigma}_{(lm)} = \vec{\sigma}_l - \vec{\sigma}_m \text{ with } \vec{\sigma}_l \cdot \vec{\sigma}_m = 0$$

hydrostatic pressure:
volume change
without distortion
(if bulk modulus isotropic)

pure shear stress:
distortion
without volume change

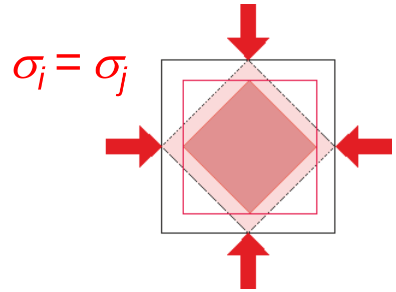

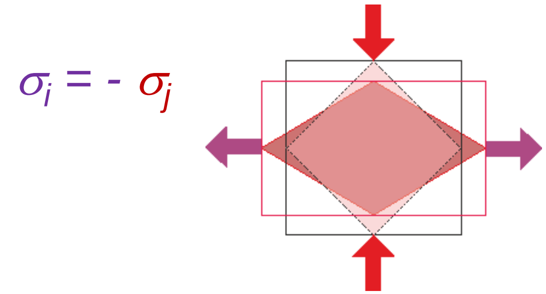

Shear stresses in $CeCu_{5.9}Au_{0.9}$

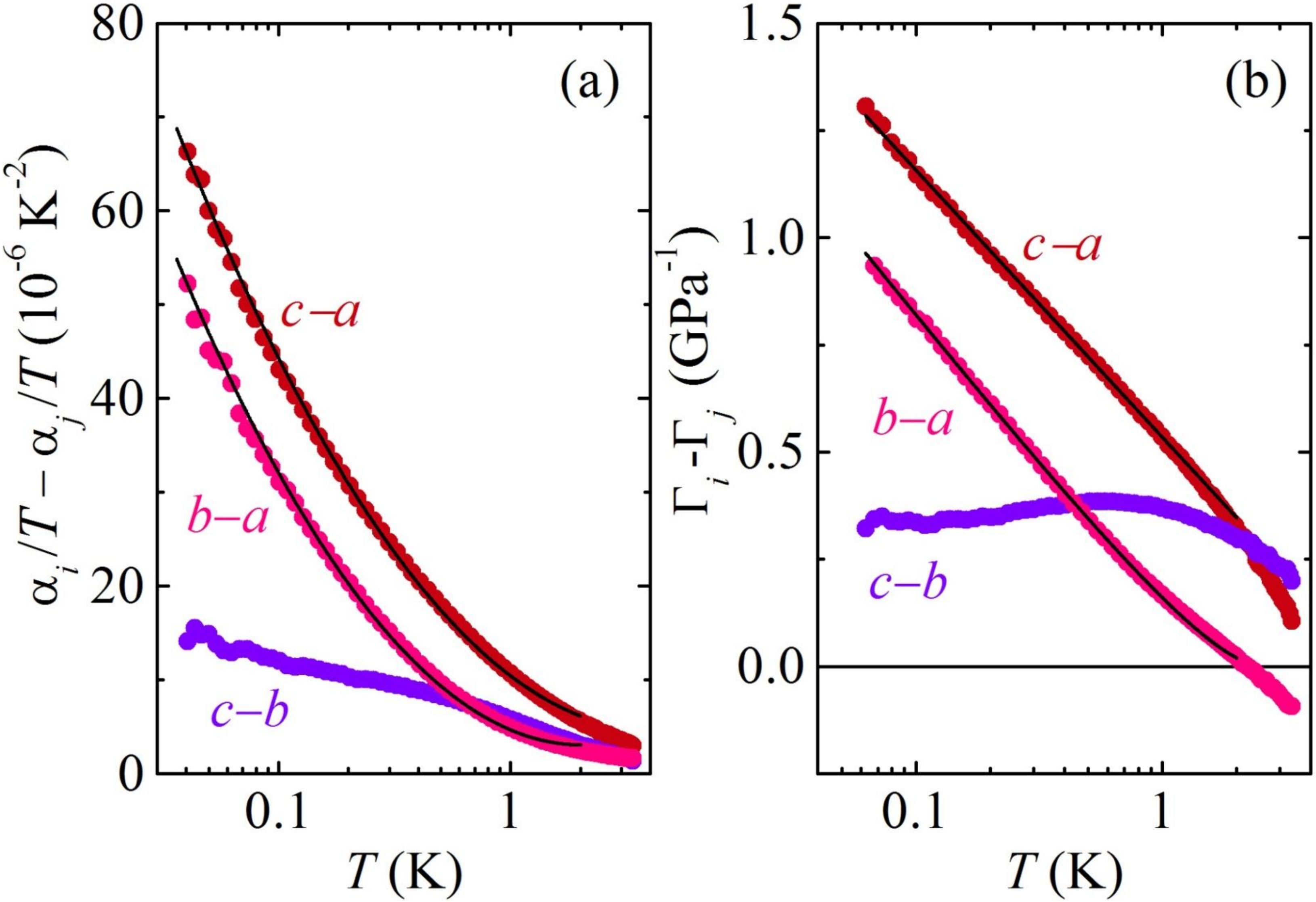

Measuring the stress dependence of the entropy

$$\vec{\nabla} S = (\partial S/\partial\sigma_a, \partial/\partial S\sigma_b, \partial S/\partial\sigma_c)$$

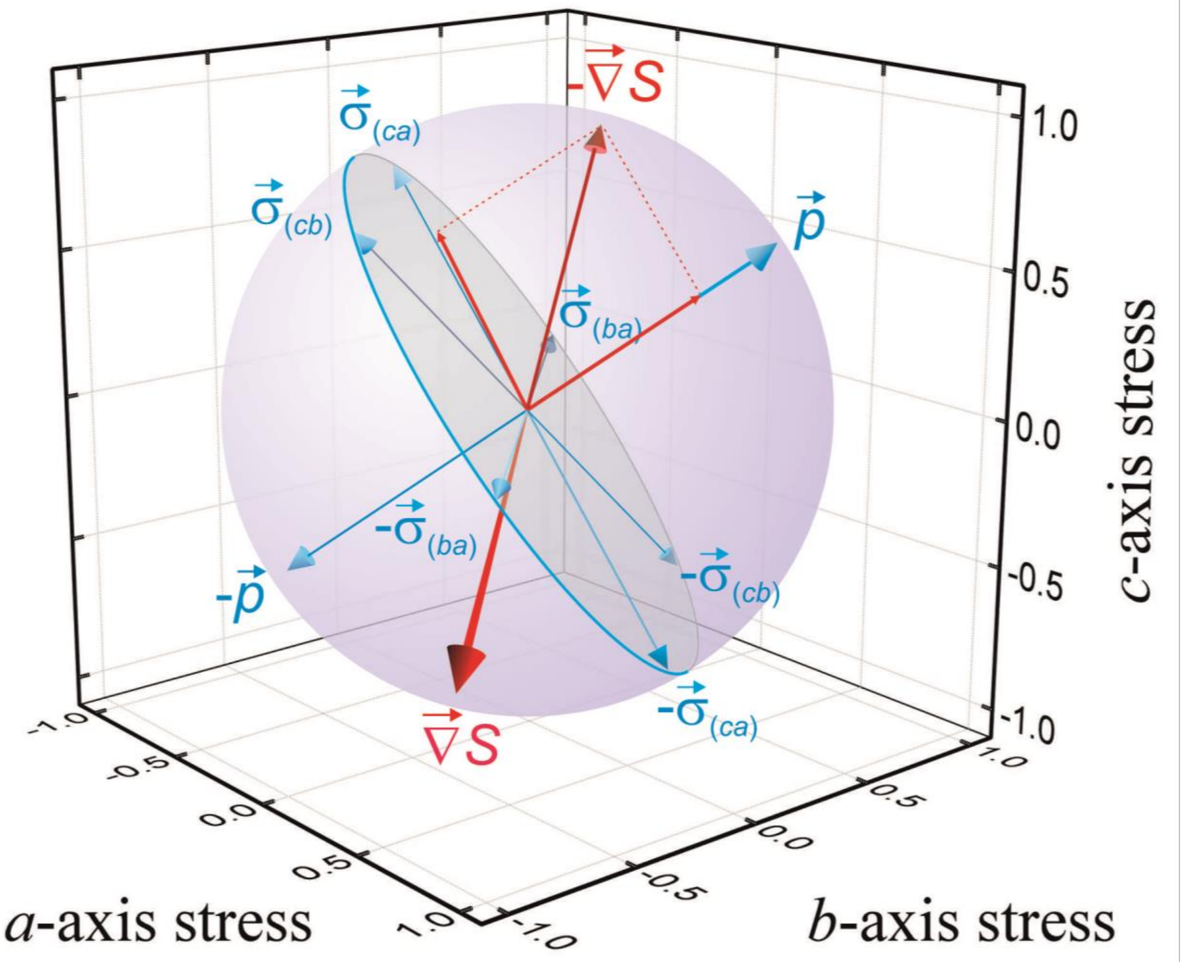

Anisotropic stress dependence of the entropy in $CeCu_{5.9}Au_{0.1}$

steepest slope of *S*, pointing to the closest maximum of *S*, i.e., a QCP

pure shear stress contribution

hydrostatic pressure contribution

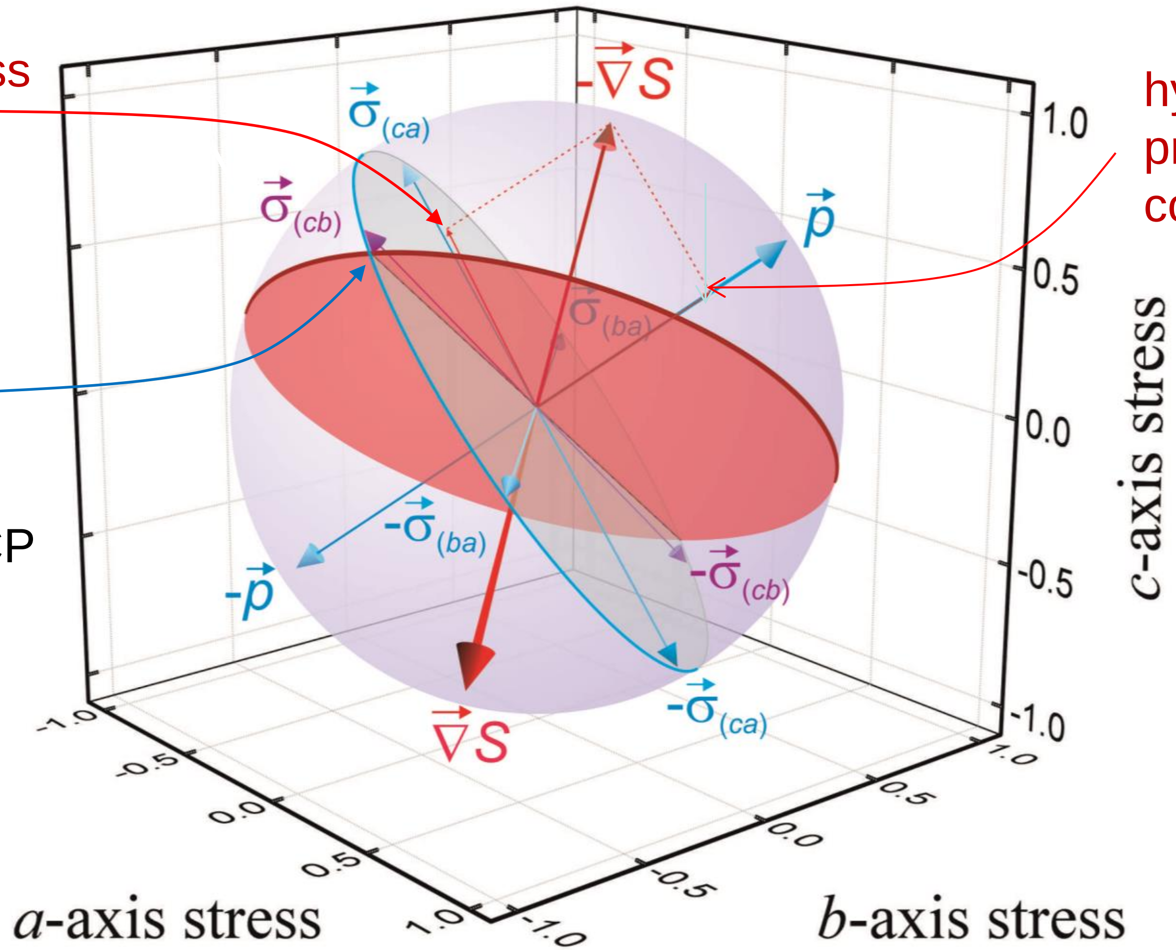

$\vec{\sigma}_{(cb)}$ nearly $\perp$ $\vec{\nabla}S$.

does not change distance to the QCP

Summary: stress combinations driving the QCP in $CeCu_{5.9}Au_{0.1}$

$\Gamma_{(ij)}$ (GPa^{-1}) for $|\vec{\sigma}|, |\vec{p}| = 1$

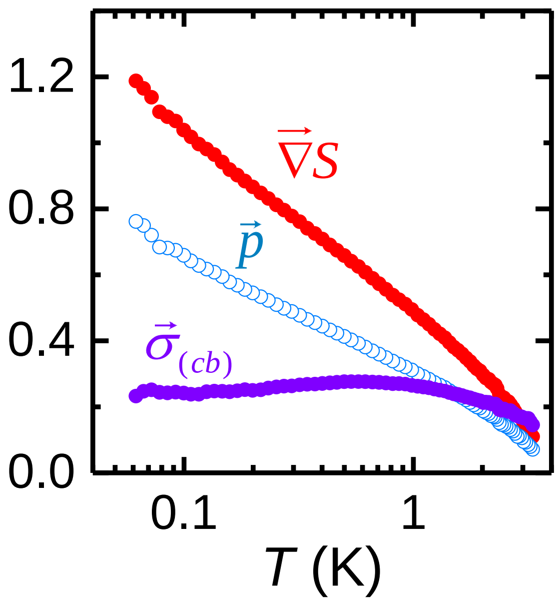

Pictorial illustration of the entropy landscape for a 2D system

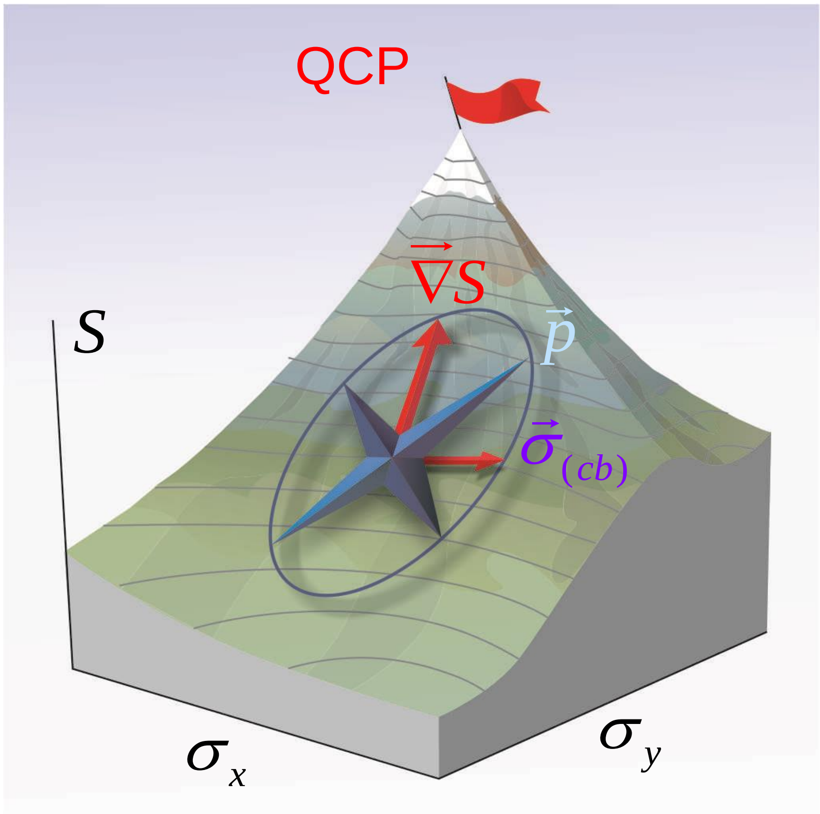

What is the signiificance of the direction of the pure shear stress $\sigma_{(ca}$ enhancing

Relation of stress anisotropies to quantum critical fluctuations?

Inelastic fluctuations (ħω = 0.1 meV) in the *a*c** plane

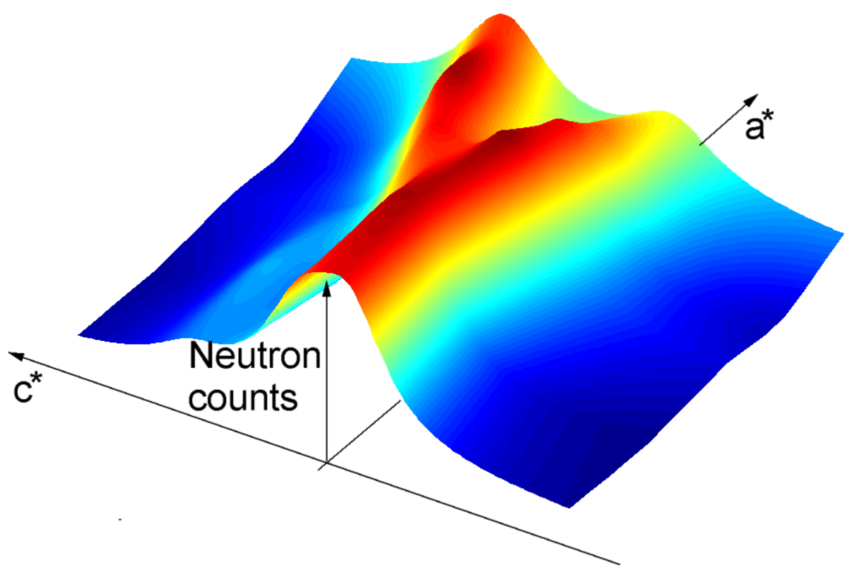

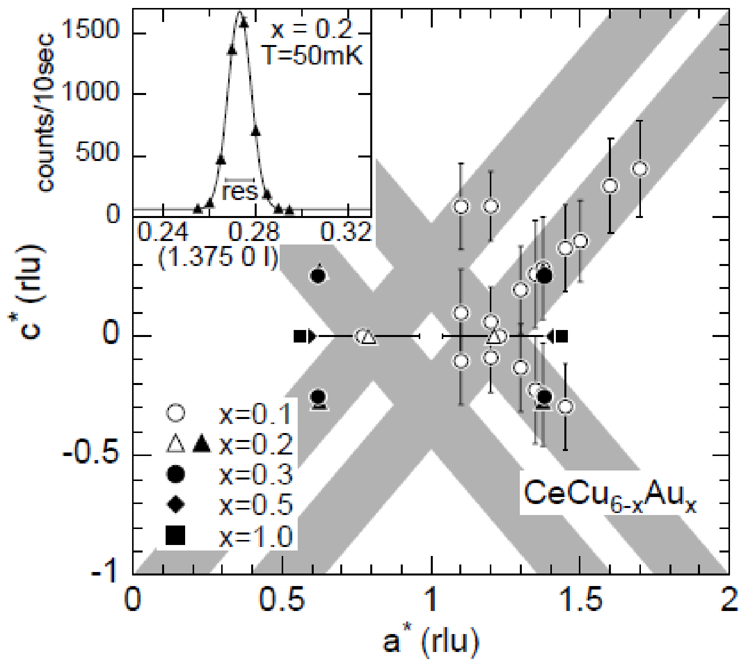

Pure shear stress $\sigma_{(ca)}$ tilts the planes of quantum-critical AF fluctuations

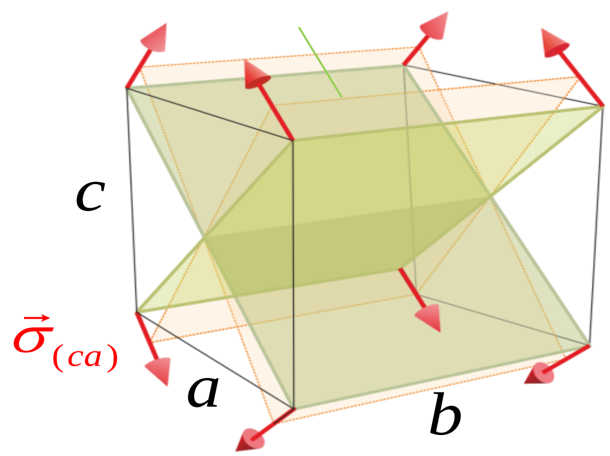

Anisotropic uniaxial pressure dependence of T_N for $CeCu_{5.8}Au_{0.2}$

Specific heat under hydrostatic …

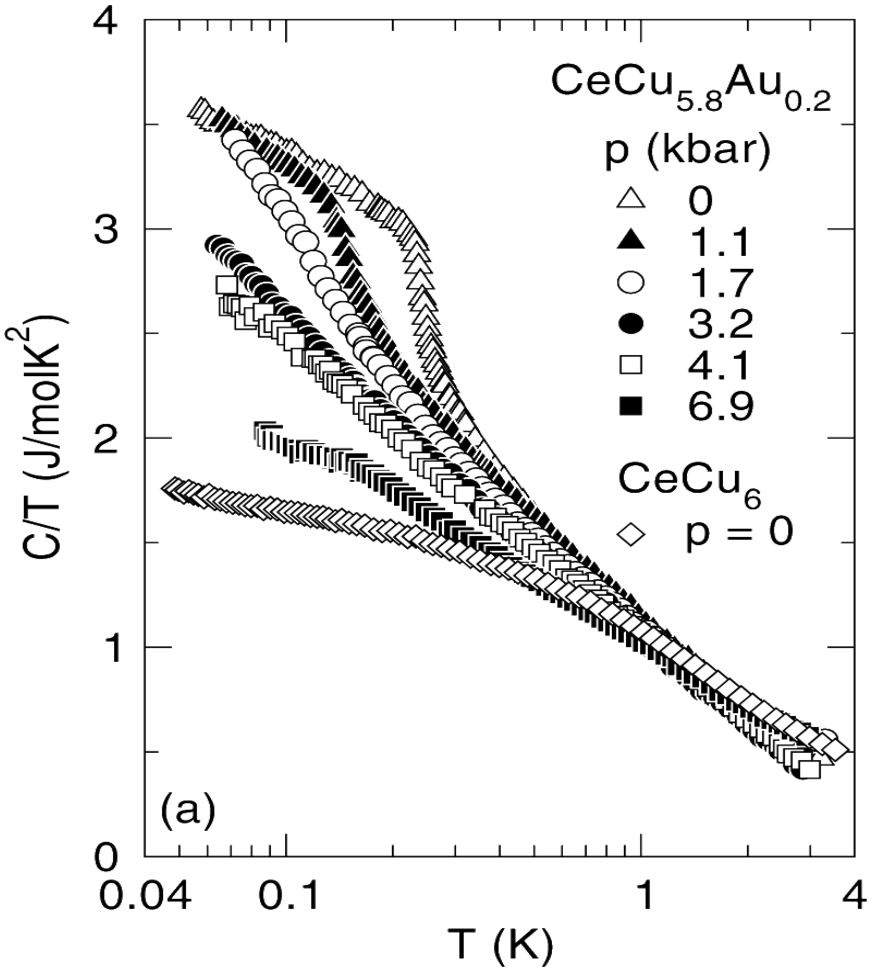

… and uniaxial pressure

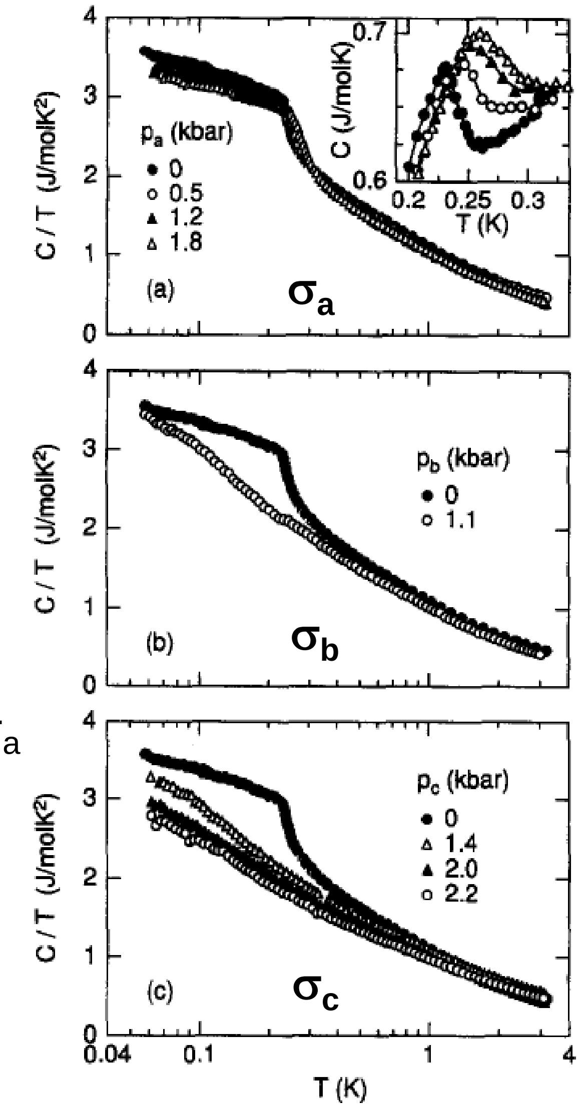

Decrease of T_N under hydrostatic pressure and uniaxial pressure for σ_b and σ_c

Increase for σ_a

HvL et al., PRB 63, 134411 (2001)
*M. Sieck et al., Physica B **230,** 583 (1997)*

Pressure vs. volume – stress vs strain in $CeCu_{5.9}Au_{0.1}$

Strong anisotropy of $T_N(\sigma_i)$

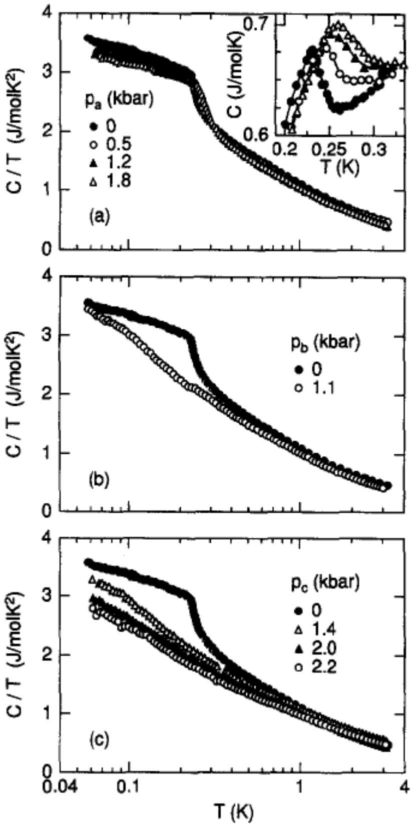

Stress Grüneisen parameters

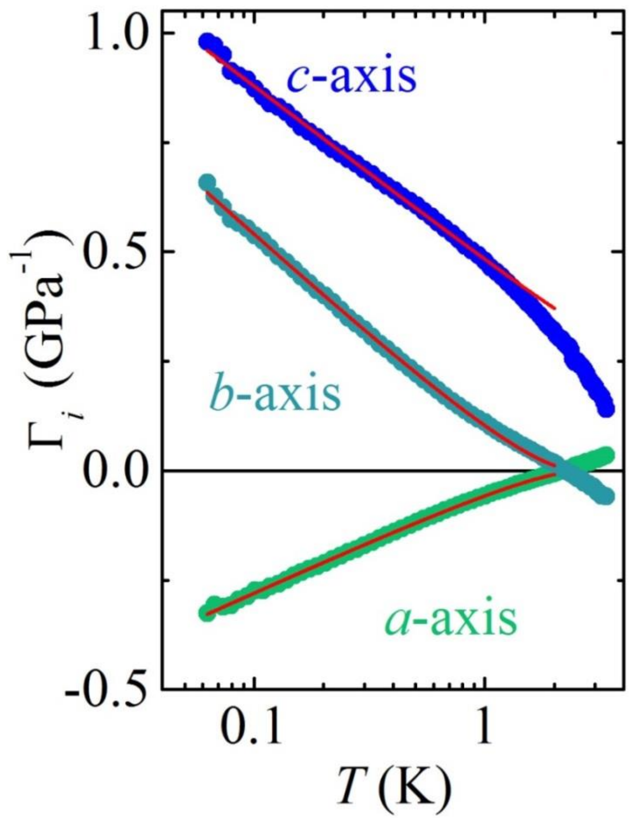

Strain Grüneisen parameters

$$\Gamma_i^{(\epsilon)}(\epsilon_i) = \sum_{j=1}^{3} c_{ij}\Gamma_j$$

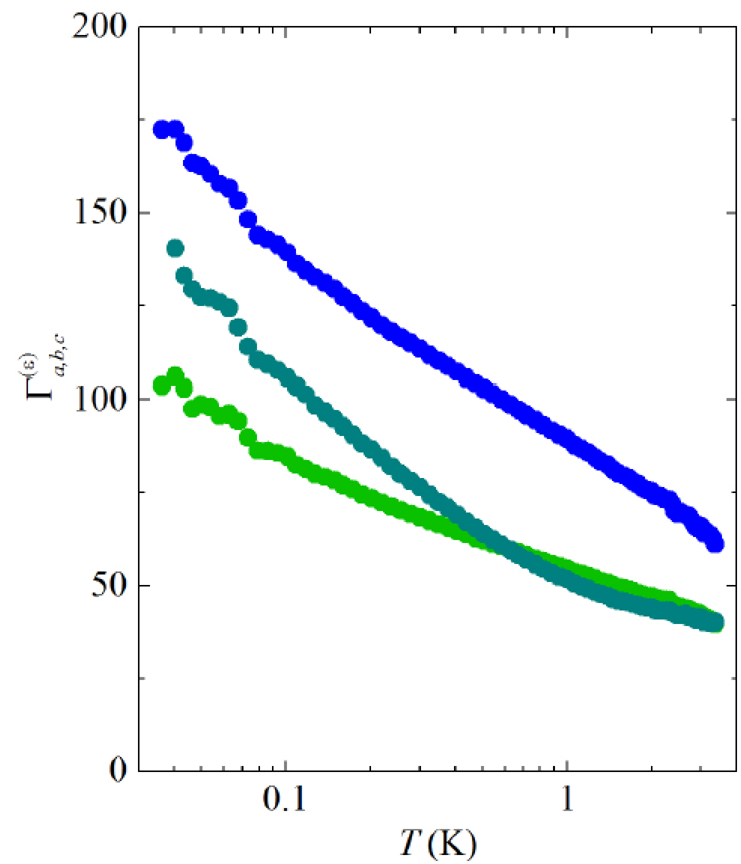

Does the monoclinic-orthorhombic transition qualify as a QPT?

Orthorhombic-monoclinic transition (T_m = 220 K in $CeCu_6$)

T_m and the monoclinic angle (2 ° in $CeCu_6$) decrease rapidly with Au concentration

Proximity to magnetic QCP : Coupling of two ordering phenomena, tetracritical point?

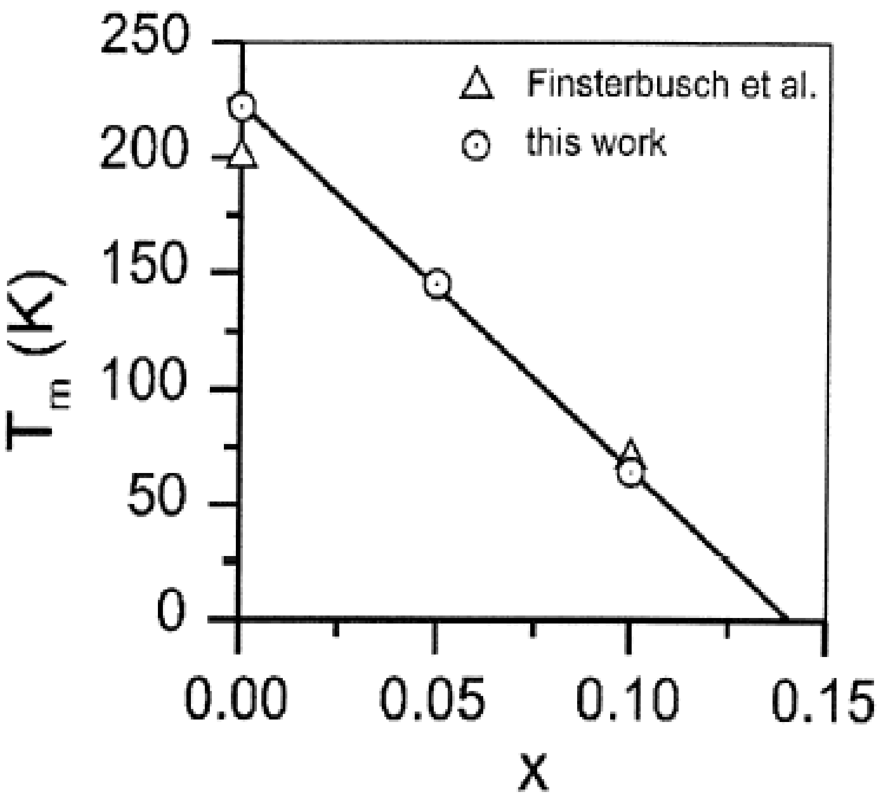

Grube et al., PRB 1999

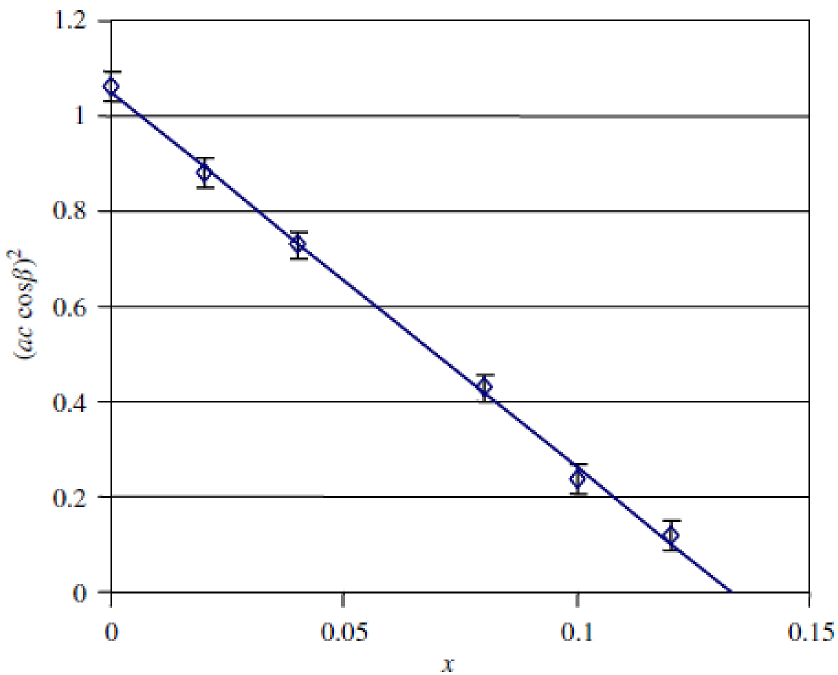

Robinsen et al., Physiba B 2006

Observation of the monoclinic splitting in $CeCu_{5.95}Au_{0.05}$ with elastic neutron scattering

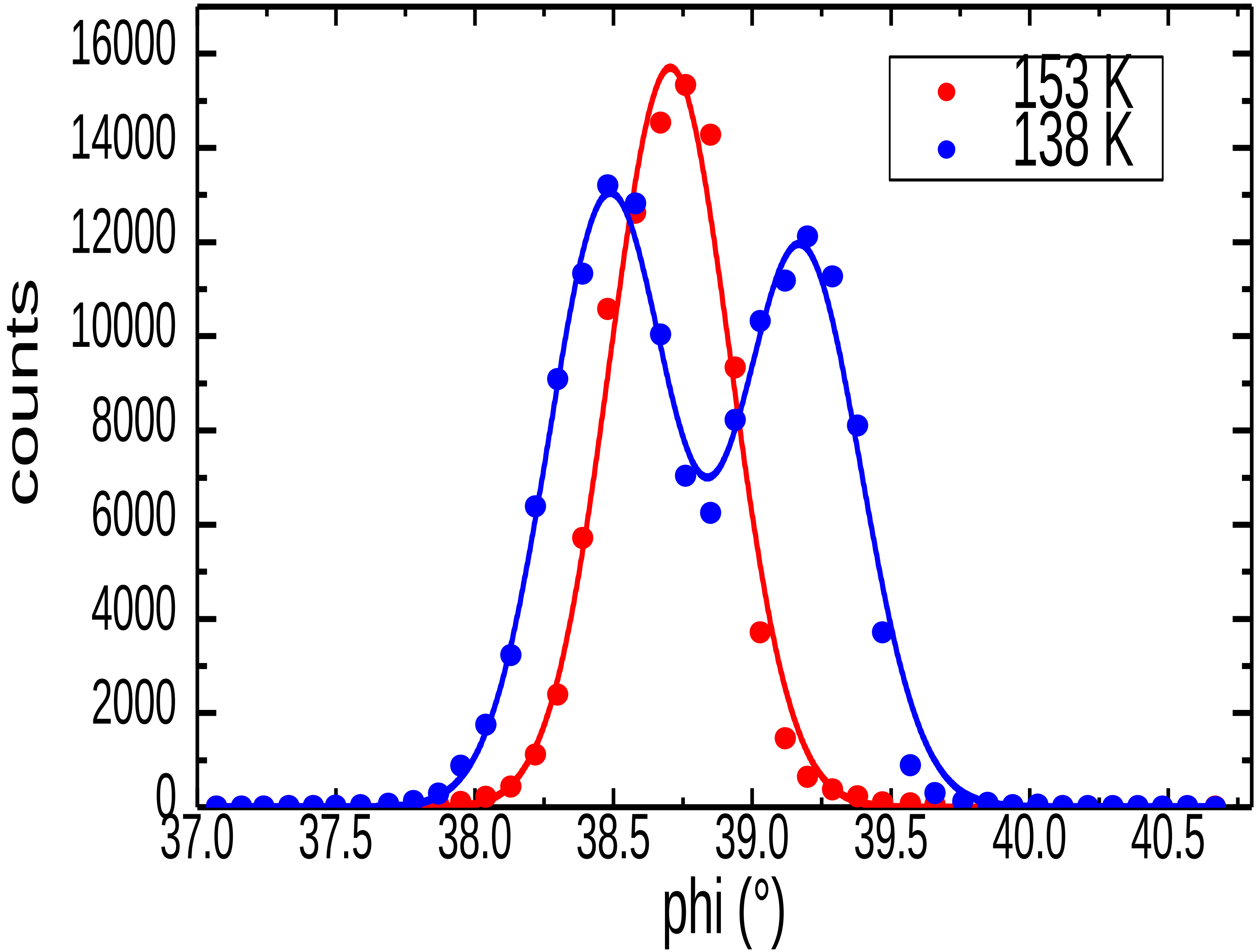

Observation of the monoclinic splitting in $CeCu_{5.95}Au_{0.05}$ with elastic neutron scattering

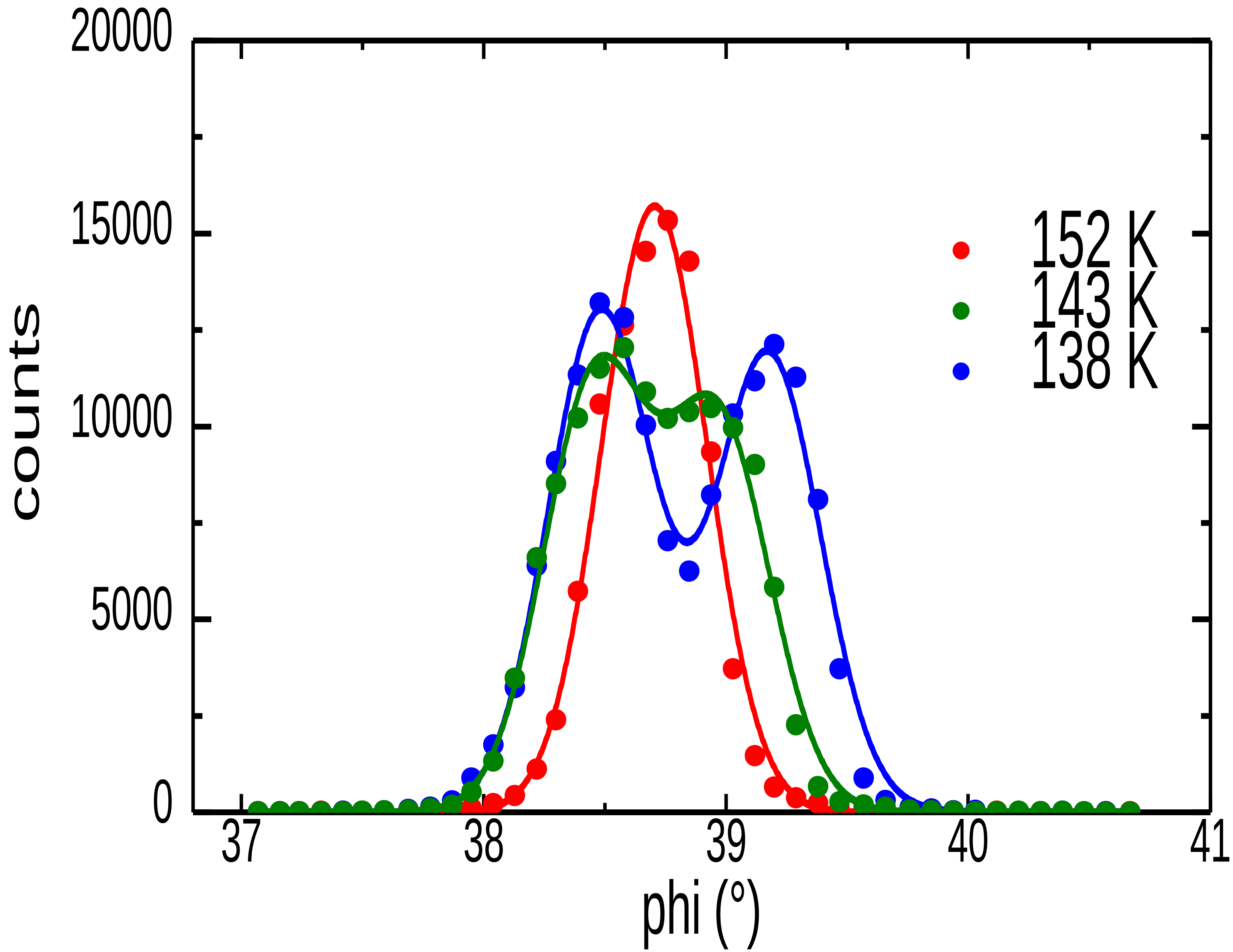

Temperature dependence of the monoclinic angle for x = 0.05

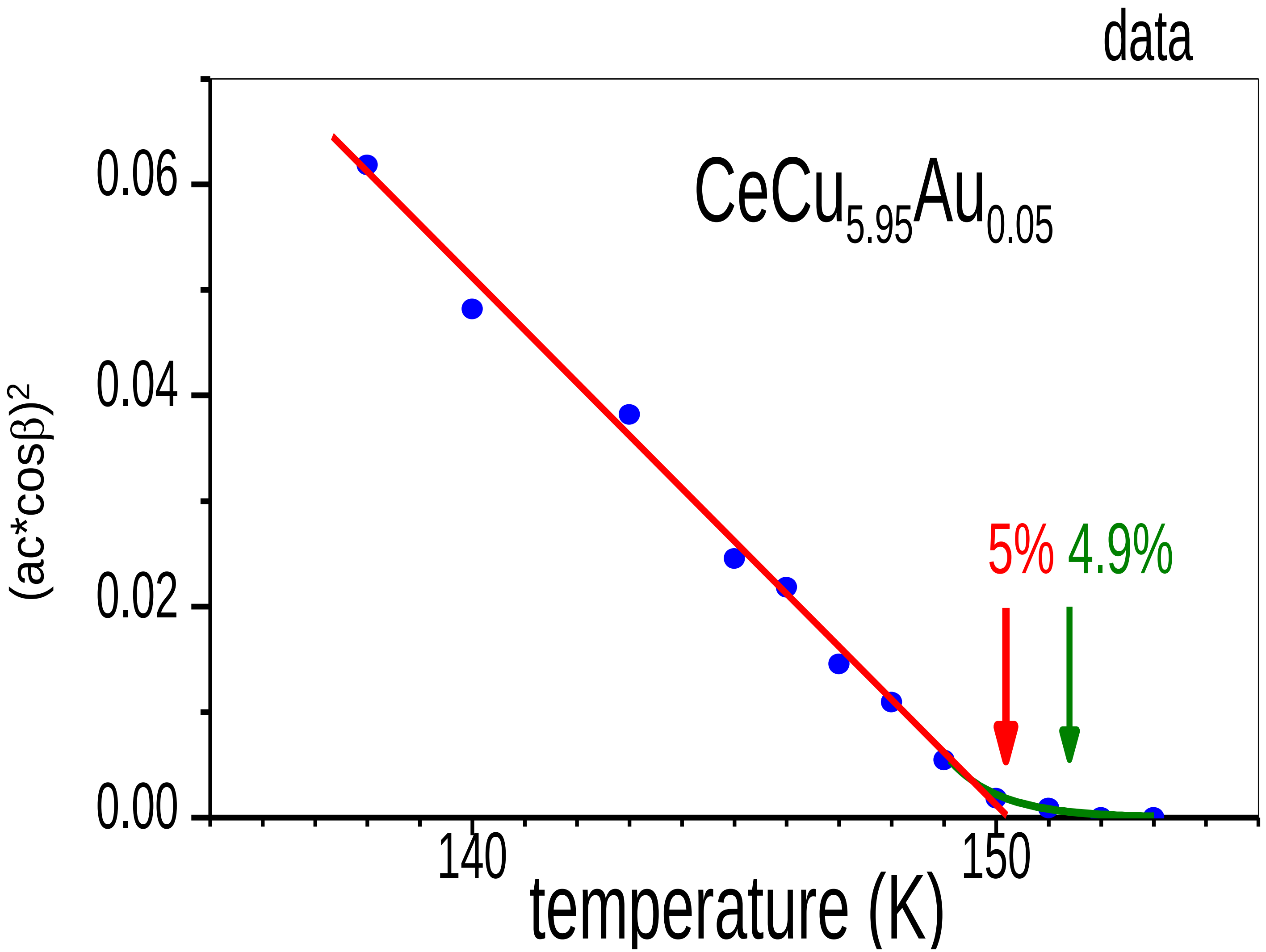

… yields, as a byproduct, an accurate check of the composition homogeneity

Temperature dependence of the monoclinic angle for $x = 0.1$

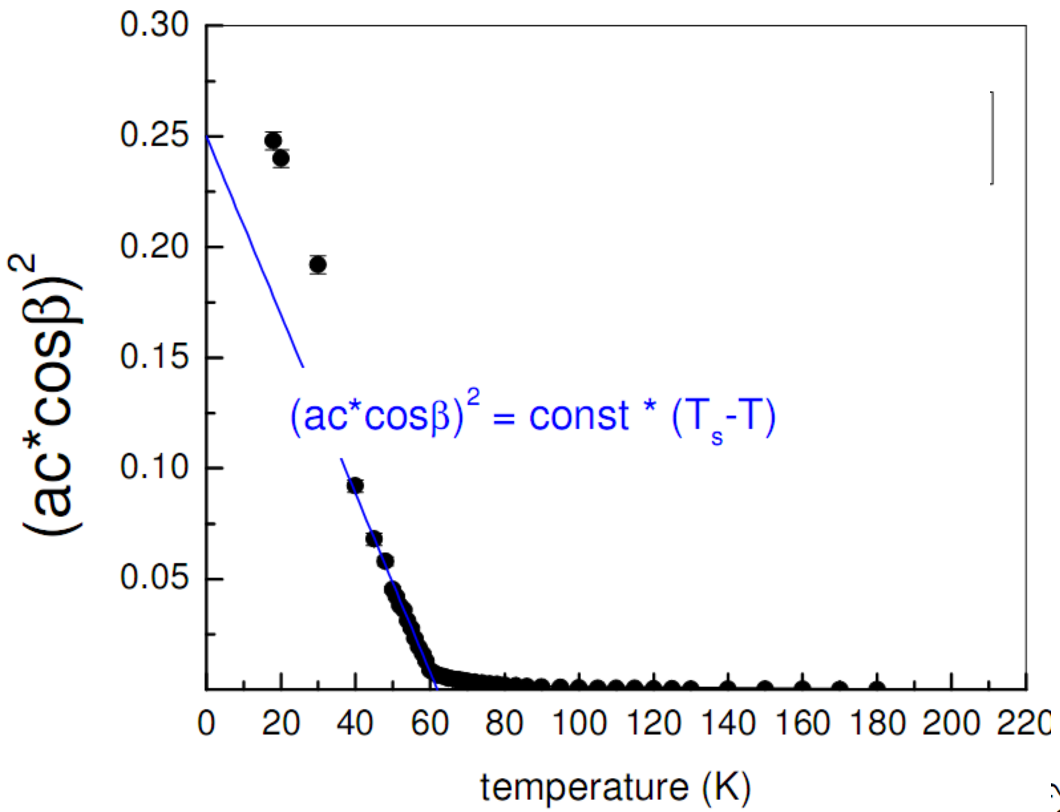

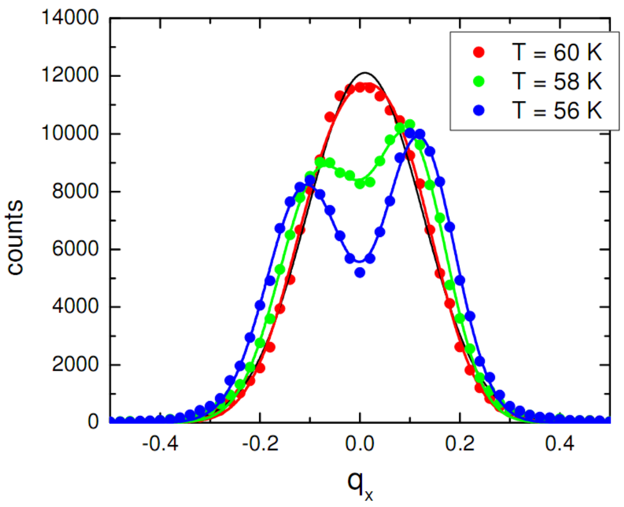

Extended high-temperature tail of the order parameter, decaying exponentially

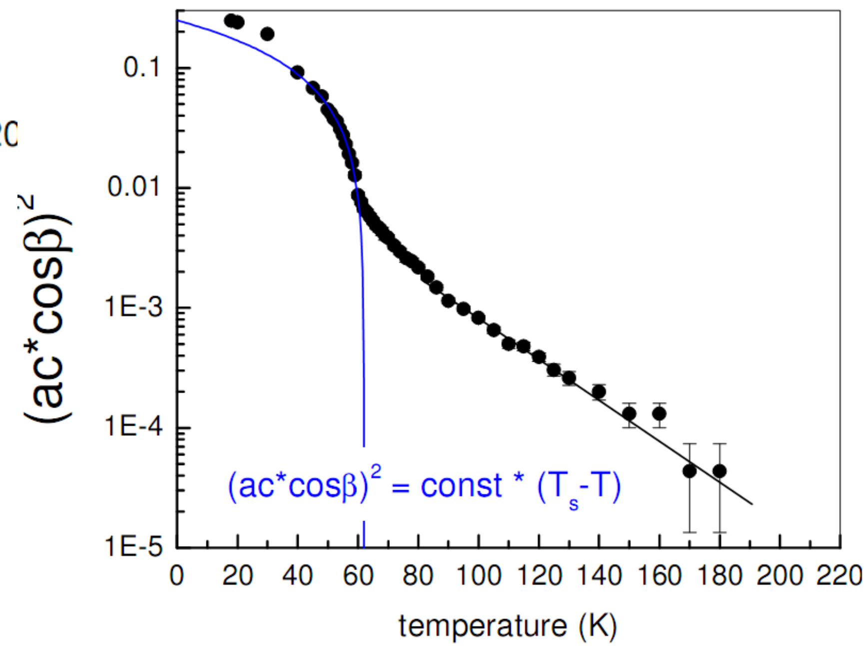

Data for samples close to the structural transition $T_m \rightarrow 0$

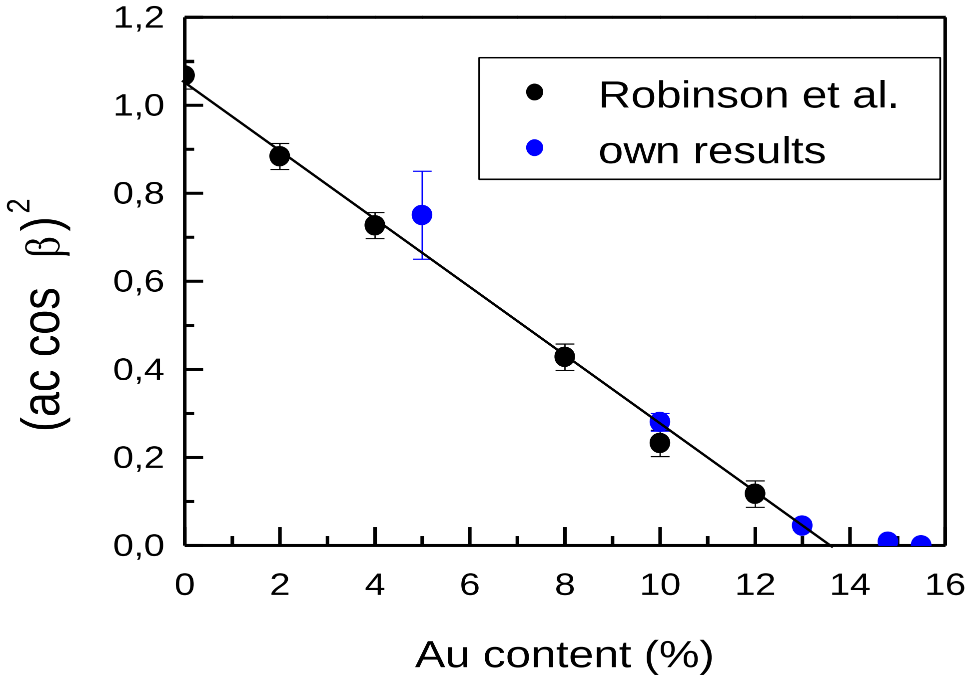

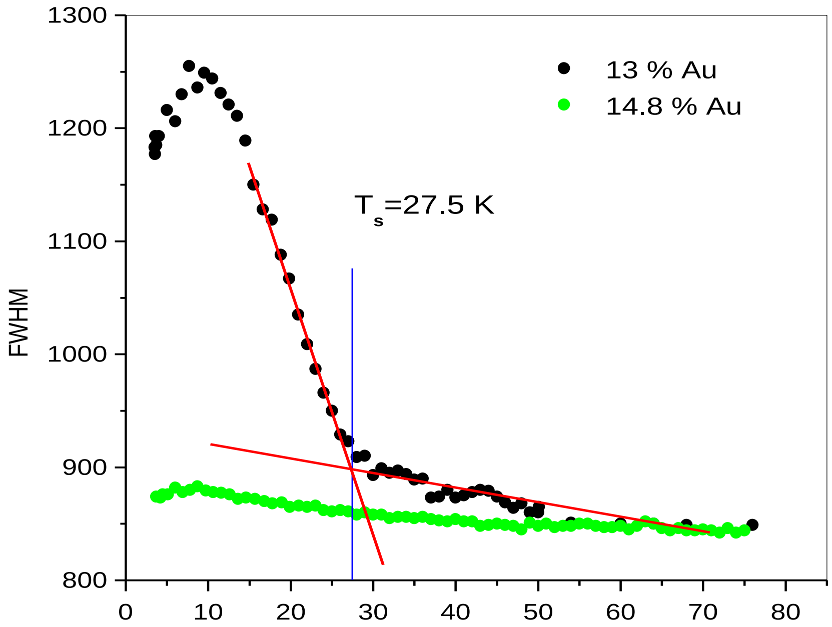

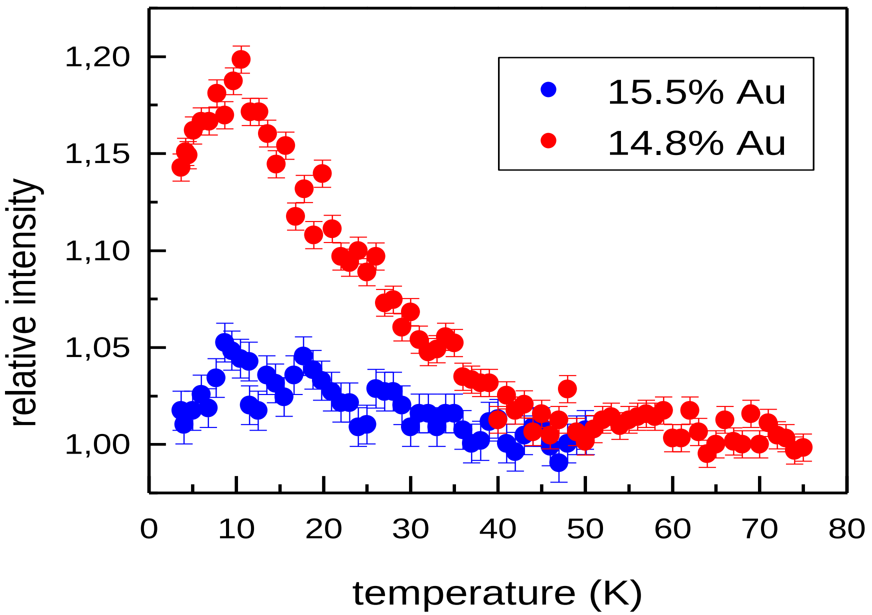

High-temperature tail prevails even for samples where no structural transition occurs

Observation of a maximum of the structural order parameter around 8 K (~ T_K)

Considering the effect of hydrostatic pressure

Hydrostatic pressure suppresses monoclinic and AF phases alike:
Suppression of AF will not restore monoclinic phase

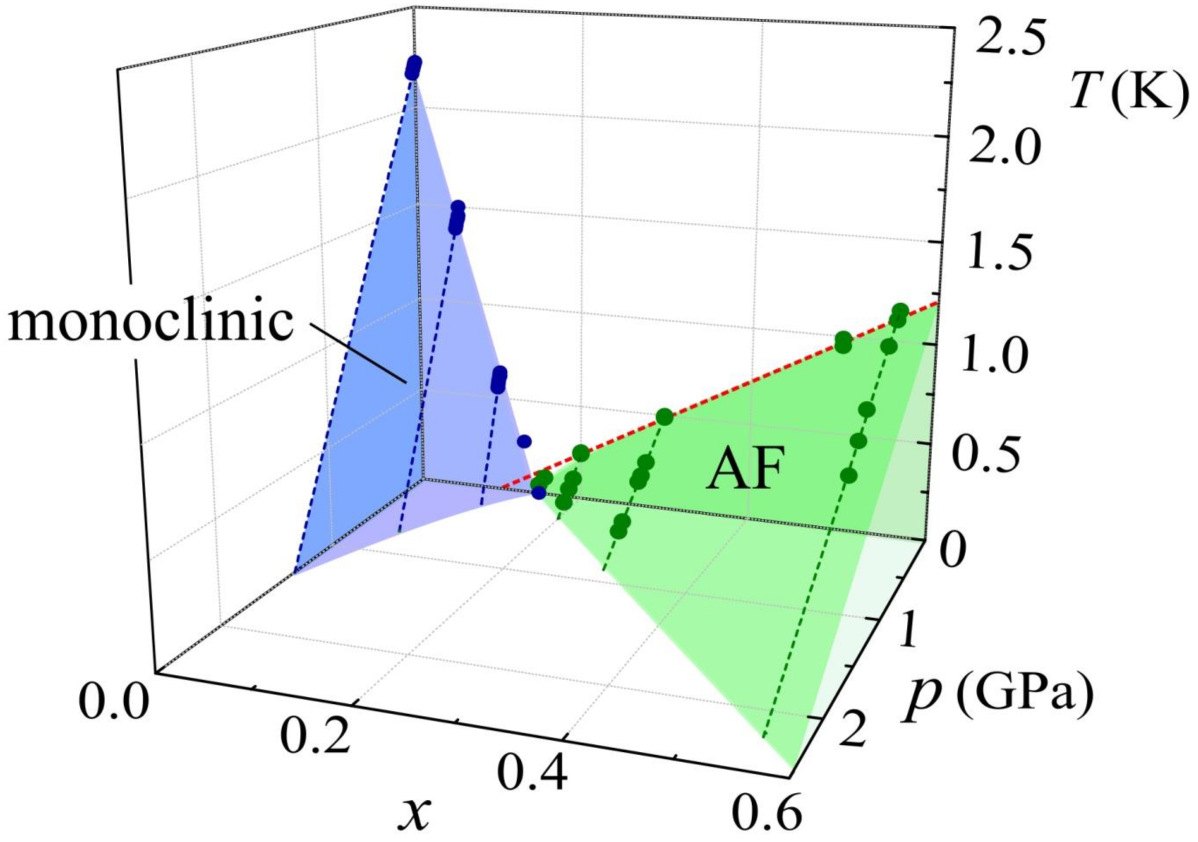

Monoclinic distortion is only accidentally “coupled“
to magnetic QCP at ambient pressure